X-751-70-369
PREPRINT

NASA TM X- 65371

ATS-V MILLIMETER WAVE EXPERIMENT DATA REPORT, VOL. II JANUARY-AUGUST 1970

LOUIS J. IPPOLITO

OCTOBER 1970

GSFC
GODDARD SPACE FLIGHT CENTER
GREENBELT, MARYLAND

X-751-70-369

ATS-V MILLIMETER WAVE EXPERIMENT DATA REPORT, VOL. II JANUARY-AUGUST 1970

Louis J. Ippolito
Communications R&D Branch

October 1970

Goddard Space Flight Center
Greenbelt, Maryland

ATS-V MILLIMETER WAVE EXPERIMENT DATA REPORT, VOL. II JANUARY-AUGUST 1970

Louis J. Ippolito
Communication R&D Branch

ABSTRACT

The Applications Technology Satellite (ATS-V) Millimeter Wave Propagation Experiment is the first flight experiment in the NASA Goddard Millimeter Wave Measurements Program for the determination of long- and short-term attenuation statistics of operational millimeter wavelength earth-space links as a function of defined meteorological conditions. The ATS-V Experiment, launched August 12, 1969, is providing the first propagation data from an orbiting geosynchronous spacecraft in the 15 GHz (downlink) and 32 GHz (uplink) frequency bands. Several stations in the continental U.S. and Canada have been operating with the downlink transmission from the satellite since late September 1969.

This report updates measurements reported in the first Data Report (X-733-70-123) and provides the first results of high rainfall measurements at the NASA Rosman station.

The spacecraft transmitter is an all solid state phase modulated unit that provides up to 250 MW of CW power at 15.3 GHz. The 31.65 GHz uplink signal is derived from a frequency stabilized klystron, varactor upconverter, and 1000 watt traveling wave tube amplifier. A multi-level computer processing program generates propagation statistics for attenuation as a function of rainfall rate, sky temperature, radar backscatter, and other meteorological variables.

Downlink measurements made at the NASA Rosman, North Carolina Station typically show attenuations of 1 to 3 db in light rains or dense fog; 3 to 7 db in continuous rains (5 to 50 mm/hr.), and a number of fades exceeding 12 db in heavy thunderstorms. Uplink fades of up to 18 db in heavy rains have been observed.

Correlation of measured attenuation with ground measured rainfall rate was low for a single gauge but improved significantly with height averaging of 10 gauges.

Correlation of measured attenuation with sky temperature recorded on a small aperture radiometer was very good for most storms. Valid predictions of attenuation from 16 GHz sky temperature measurements were observed for up to 15 db of measured attenuation.

The uplink to downlink attenuation ratio varied with each precipitation event and often varied during a single storm. The ratio has ranged from 2:1 to 4:1 during heavy precipitation periods.

CONTENTS

ATS-V MILLIMETER WAVE EXPERIMENT DATA REPORT, VOL. II JANUARY-AUGUST 1970

1.0 INTRODUCTION

The recent history of radio communications has been characterized by a continual extension to higher and higher frequency bands to support the increasing data handling requirements of an expanding technology. The commonly utilized frequency bands below 10 GHz which support virtually all terrestrial communications links were further stressed with the relatively recent advent of space communications.

The frequency bands between 10 and 300 GHz, commonly called "millimeter waves," offer a promising area for reducing the overcrowded situation in the lower bands. In addition to relieving spectrum crowding, millimeter wave systems offer extremely wide bandwidth capabilities, high gain-small aperture antenna characteristics, and reduced size and weight of components.

The first three "windows" in the electromagnetic spectrum above 10 GHz where water vapor and oxygen absorption are low occur at frequencies below 19 GHz, at 35 GHz, and at 94 GHz. It is in these bands that the greatest potential for earth-space applications exist, but propagation data is required by the systems designer before performance characteristics can be predicted and evaluated.

A Millimeter Wave Propagation Experiment was launched aboard the Applications Technology Satellite (ATS-V), on August 12, 1969, and is providing the first propagation measurements from an orbiting satellite in the Ku (12.5 to 18 GHz) and Ka (26.5 to 40 GHz) frequency bands. The prime objective of this experiment is to provide sufficient information on the propagation characteristics of the Earth's atmosphere so that this relatively unexplored and unused portion of the electromagnetic spectrum can be most effectively utilized for communications and data handling applications.

The ATS-V Millimeter Wave Experiment is providing amplitude and phase measurements on two independent test links at 15.3 GHz (satellite-to-earth) and at 31.65 GHz (earth-to-satellite) during measured and defined meteorological conditions. Several stations in the continental U.S. and Canada have been operating with the satellite transmission since October 1969.

This paper will briefly describe the overall experiment configuration and present data results from the first 10 months of measurements made at the NASA/GSFC station, located at Rosman, North Carolina.

Reported results from other participating stations are listed in Appendix A.

1.1 Experiment Configuration

The test signal for both the uplink and downlink consists of a carrier and two sidebands equally displaced on either side of the carrier. For the uplink, the sidebands can be set at one of the discrete values ±1.0, ±10 or ±50 MHz from the 31.65 GHz carrier. For the downlink, the sidebands can be set to ±0.1, ±10 or ±50 MHz from the 15.3 GHz carrier.

Downlink measurements of carrier amplitude, upper and lower sideband amplitude, and relative sideband phase are recorded at the participating sites on magnetic tape and paper charts. Uplink measurements are performed on-board the satellite and telemetered to an ATS tracking station (Rosman, N.C. or Mojave, Calif.) for reduction and processing.

NASA operationally supports five stations which provide a representative sample of the predominate weather profiles in the continental U.S. These stations are:

1. The NASA/GSFC Transportable Station located at Rosman, North Carolina, (receive and transmit capability).

2. The Naval Electronics Laboratory Center (NELC), La Posta, Calif. (receive capability).

3, 4. Ohio State University (OSU), Columbus, Ohio (two receive sites on variable base line for spatial diversity tests).

5. University of Texas, (U of T), Austin, Texas (receive capability).

In addition, a number of independent experimenters have expressed interest in participating in downlink measurements with the ATS-V satellite. Table 1 lists all of the stations presently equipped to operate with the ATS-V Millimeter Wave Experiment, in order of increasing elevation angle. A number of pairs of stations are available for diversity evaluation with baselines of 2 to 27 miles in length. The OSU mobile is designed for variable baseline measurements described in another paper, (Ref. III-1, Appendix A).

Figure 1 presents the basic components of the ATS-V Millimeter Wave Propagation Experiment. The spacecraft hardware consists of the 31.65 GHz receiver-signal processor, the main 15.3 GHz transmitter, and a 15.3 GHz "back-up" CW receiver, all interfacing with the ATS-V Spacecraft telemetry and command subsystems.

Table 1
ATS-V Millimeter Wave Experiment Participating Stations

STATION		LATITUDE (NORTH)	LONGITUDE (WEST)	NOMINAL ELEVATION ANGLE	ANTENNA SIZE	RECEIVER TYPE
AIR FORCE CAMBRIDGE RESEARCH LABS, BEDFORD, MASS.		42°23'	71°15'	30°	28 FT.	MCW
DEPT. OF TRANSPORTATION, CAMBRIDGE, MASS.		42°36'	71°29'	30°	10 FT.(2)	SB
COMMUNICATIONS RESEARCH CENTRE, OTTAWA, CANADA	PRIME SITE	45°21'	75°54'	30°	30 FT.	SB
	SECOND SITE				8 FT.	MCW
ROME AIR DEV. CENTER, ROME, N.Y.		43°08'	75°37'	32°	15 FT.	SB
BELL TELEPHONE LABORATORIES, HOLMDEL, N.J.		40°23'	74°11'	34°	20 FT.	CW
U.S.A.S.C.A., LAKEHURST, N.J.		40°00'	74°25'	34°	30 FT.	MSB
COMMUNICATIONS SATELLITE CORP., CLARKSBURG, MD.		39°12'	77°16'	36°	15 FT.	SB
GODDARD SPACE FLIGHT CENTER, GREENBELT, MD.	RECEIVE SITE	39°42'	76°48'	36°	15 FT.	MCW
	TRANSMIT SITE*				10 FT.	-
NAVAL RESEARCH LABORATORIES, WALDORF, MD.				36°	60 FT.	MCW
OHIO STATE UNIVERSITY, COLUMBUS, OHIO	FIXED SITE	40°00'	83°02'	39°	30 FT.	MSB▲
	MOBILE SITE				15 FT.	MSB▲
GODDARD TRANSPORTABLE STATION, ROSMAN, N.C.*		35°12'	82°53'	42°	15 FT.	MSB▲
ESSA WAVE PROP. LAB., BOULDER, COLO.		40°00'	105°16'	44°	10 FT.	MCW
WESTINGHOUSE GEORESEARCH, BOULDER, COLO.		40°00'	105°09'	44°	12 FT.	MCW
MARTIN MARIETTA CORP., ORLANDO, FLA.		28°26'	81°26'	48°	12 FT.	MSB
NAVAL ELECTRONICS LABORATORY CENTER, SAN DIEGO, CAL.		32°40'	116°26'	50°	60 FT.	MSB▲
UNIVERSITY OF TEXAS, AUSTIN, TEX.		30°23'	97°43'	54°	10 FT.(2)	MSB▲

* -TRANSMIT STATION
▲-NASA/GSFC PARTICIPATING STATION
MSB -MARTIN SIDEBAND RECEIVER
MCW-MARTIN CW ONLY RECEIVER
SB -SIDEBAND RECEIVER
CW - CW ONLY RECEIVER

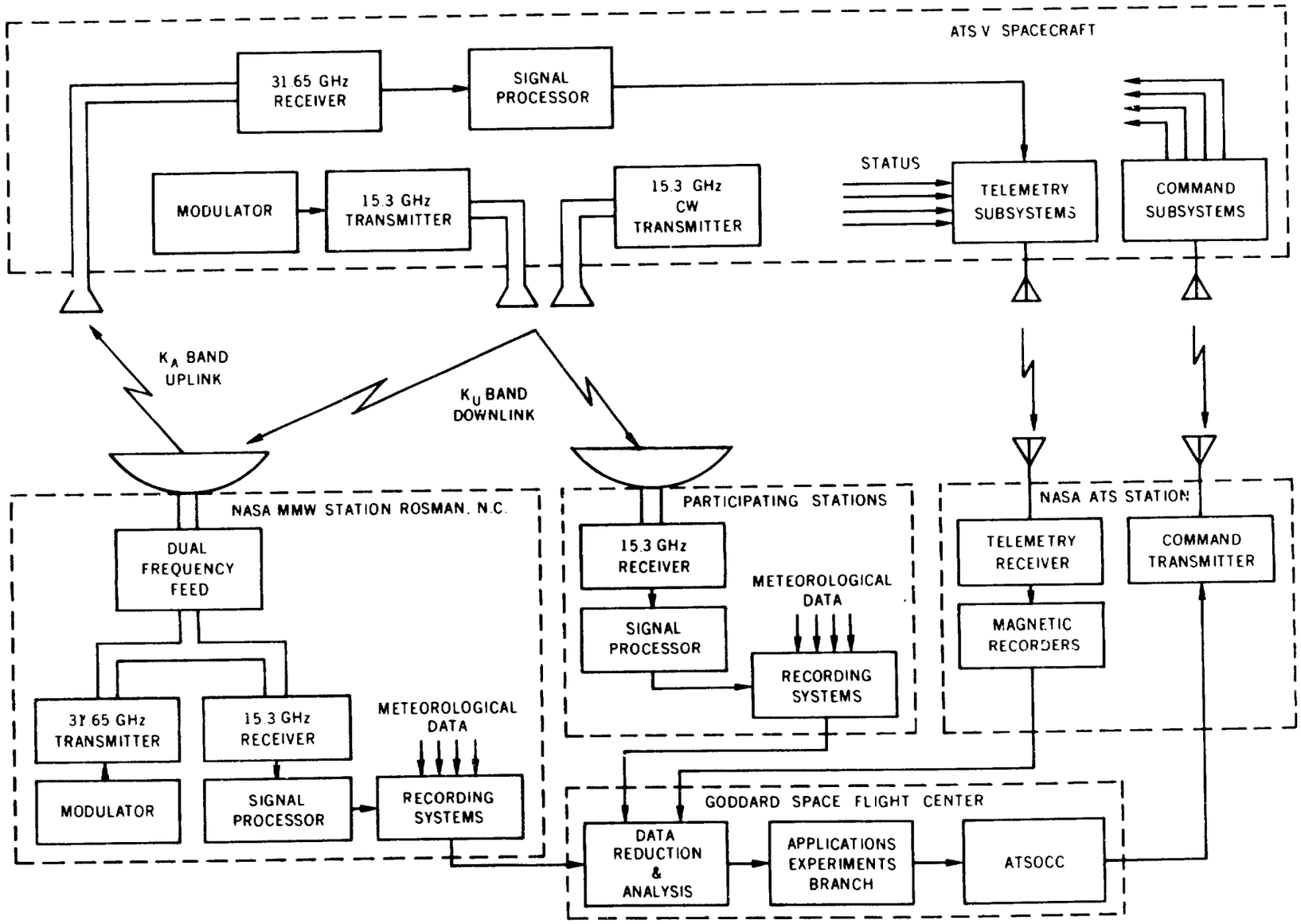

Figure 1. The ATS-V Millimeter Wave Propagation Experiment

The NASA Rosman MMW station has both a receive and transmit capability, the participating stations operate with the 15.3 GHz downlink only. Satellite telemetry, tracking and command is accomplished from either of two NASA STADAN stations, located at Rosman, North Carolina and Mojave, California. Data analysis and overall experiment management are provided by the Communications R&D Branch of Goddard's Communications and Navigation Division. Satellite and ground station interface is coordinated by the ATS Project Office through its Operations and Control Center (ATSOCC).

The Millimeter Wave Experiment flight package, built by Martin Marietta Corp., consists of four major systems; the primary 15.3 GHz transmitter, the backup 15.3 GHz transmitter (beacon), the 31.65 GHz receiver and the signal processor. The antennas for both the uplink and the downlink are linearly polarized conical horns with a full earth coverage field of view (20°, 3 db beamwidth, 19.1 db boresight gain). The horns are orthogonally aligned on the spacecraft to provide polarization isolation between the uplink and downlink.

Figure 2 shows the ATS-V Millimeter Wave Experiment flight hardware package, which consists of the main transmitter, receiver, and signal processor. The backup transmitter is a separate package with its own antenna and is identical to the main transmitter except that it does not have a modulation capability. All of the antennas are located in the center portion of the spacecraft in the earth-viewing direction. as shown in Figure 3.

The 31.65 GHz receiver utilizes a balanced mixer front end with a 17 db maximum noise figure. Maximum received signal level (in CW) is -85 dbm and minimum sensitivity is -120 dbm.

The receiver phase locks on the carrier with an aided track and search circuit with a ±5 kHz minimum pull in range over a ±320 kHz band.

The carrier amplitude, upper and lower sideband amplitudes, relative sideband phases, and VCO error voltage are produced in the signal processor and relayed to earth through the ATS-V telemetry systems.

Downlink transmitter power is 250 MW (unmodulated) and 70 MW per line (modulated), with a frequency stability of ±4 PPM per year. Thermal stability is ±3 PPM over the temperature range +4 to +38°.

The 30.6 GHz LO and the 15.3 GHz transmit carrier are both generated from a common solid-state source which starts with a 106.25 MHz crystal oscillator. The downlink modulation is accomplished at 5.1 GHz by a varactor phase modulator with the modulation index set to provide equal level carrier and first sidebands at the 15.3 GHz transmit frequency.

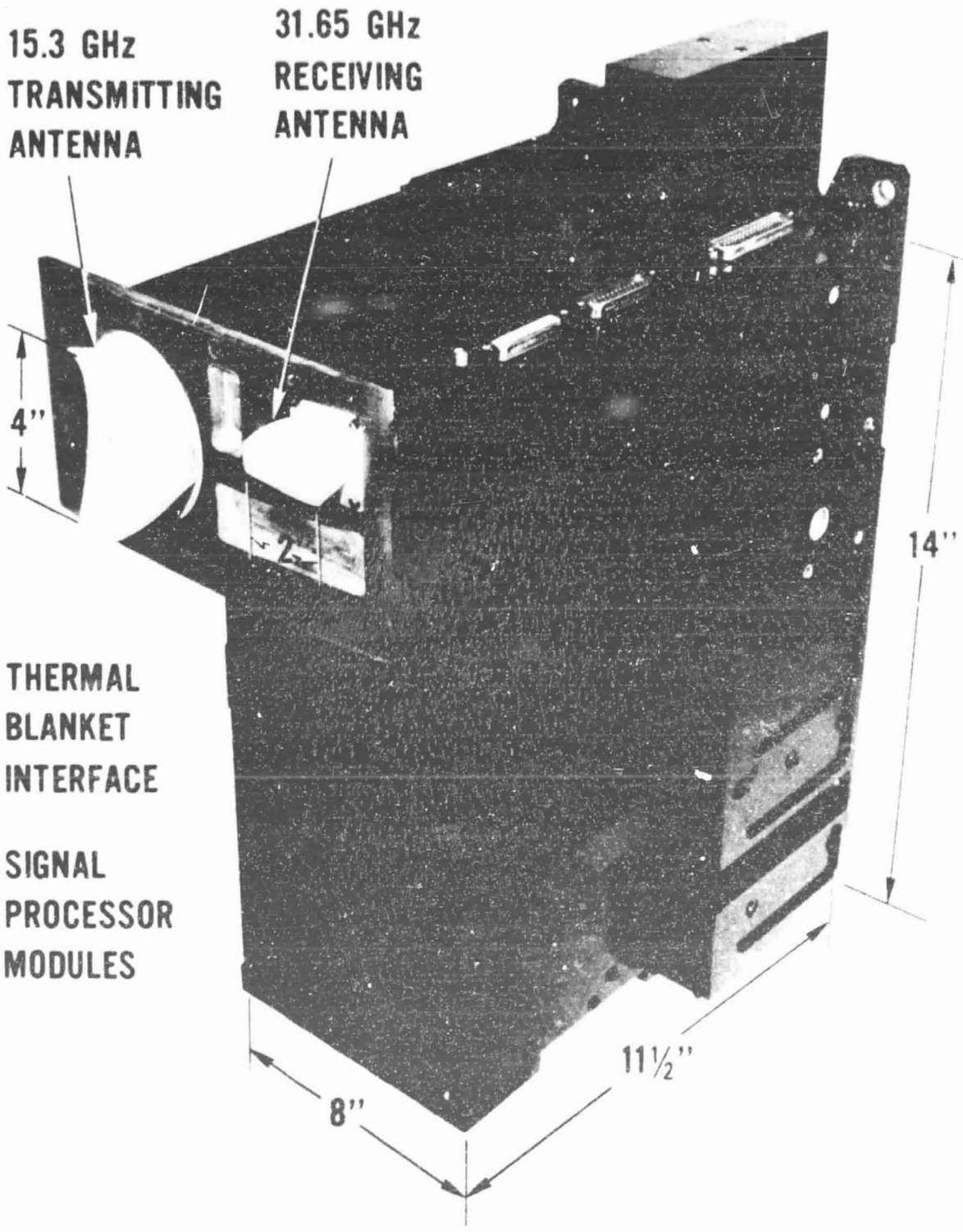

Figure 2. ATS-V Millimeter Wave Experiment Primary Flight Package

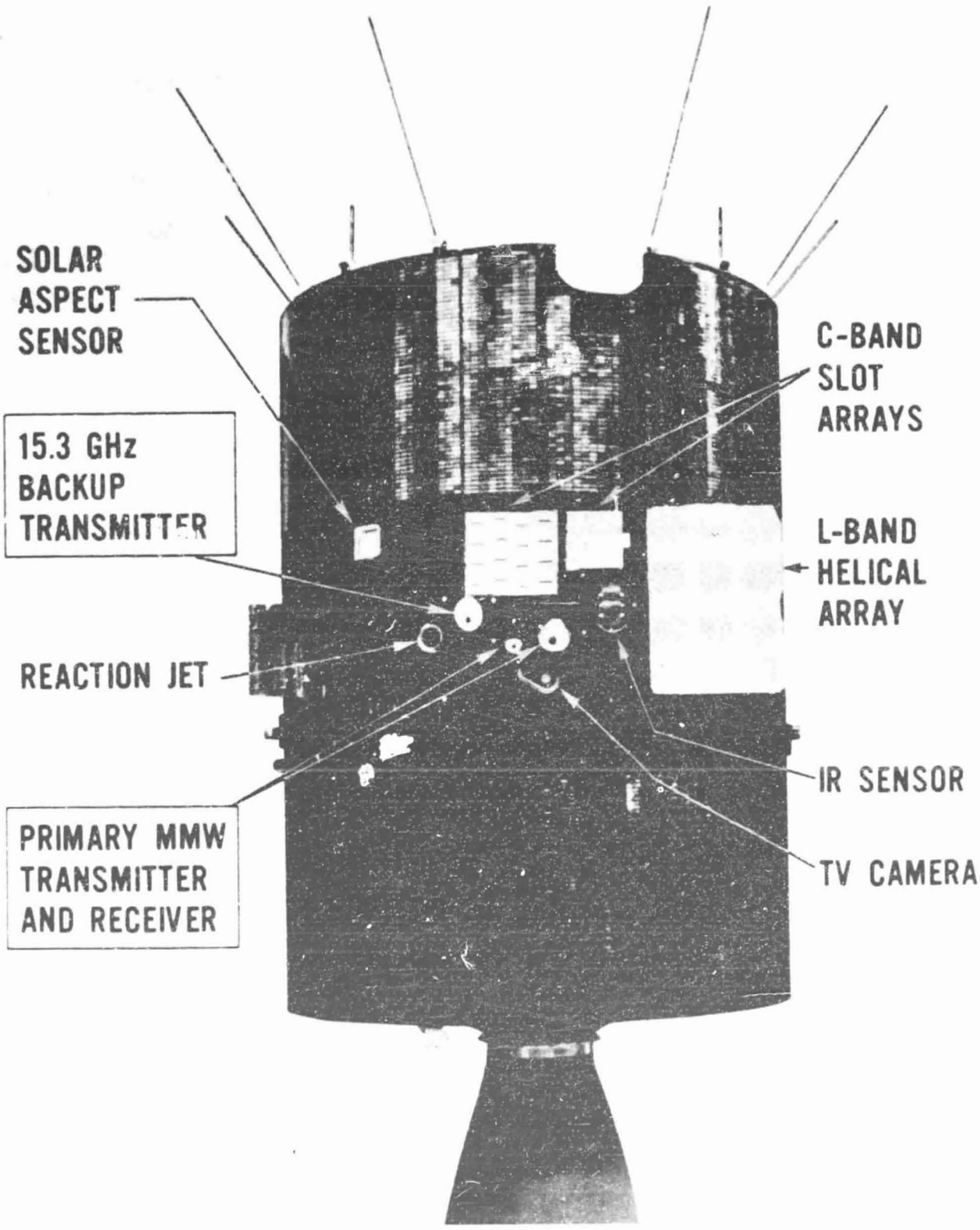

Figure 3. ATS-V Spacecraft

Detailed descriptions of the spacecraft hardware are given in references 2 and 3.

1.2 Satellite Spin Effects

The ATS-V Spacecraft was designed for geosynchronous operation at 108° West Longitude, employing a gravity gradient 3-axis stabilization system. It was successfully launched from Cape Kennedy, Florida, on August 12, 1969 on-board an Atlas-Centaur launch vehicle. During the transfer orbit phase, however, an excessive amount of fuel was expended in maintaining stabilization. The satellite was then injected to synchronous velocity at the first apogee point, rather than the second, as originally planned. The injection maneuver caused the vehicle to end up in a flat spin over the Indian Ocean with the apogee motor still attached.

The satellite drifted slowly westward with the motor attached until late in September when an attempt was made to release the apogee motor and place the vehicle at its 108° West Longitude parking position. The motor was successfully released but the spacecraft ended up with a spin in the reverse direction from that required to despin it with a yo-yo despin mechanism. The spin rate (about 76 rpm) was considered too high to safely deploy the gravity gradient stabilization booms. The satellite is still in this spin condition. Techniques to stop the spin and deploy the booms are presently under study, but full gravity gradient stabilization appears unlikely. Present plans call for operation in the spin condition until July of 1971 before any attempts will be considered to modify the spacecraft's condition.

No difficulty was encountered in acquiring the satellite signal using pointing data from the ATSOCC (ATS Operations Control Center). The phase-lock loop bandwidth of the receiver system has been adequate to lock on every pulse during high signal level conditions. The availability of 3 VCXO sweep speeds (.4, 4, and 20 .Hz/sec.) is extremely useful in maintaining lock as the signal level drops off.

The relative differential sideband phase measurement is more seriously effected by the spin than are the amplitude measurements. Errors are introduced by the doppler effects of the spinning vehicle and because of the "settling time" required of the quadrature phase detectors. Figure 4 shows an expanded time scale display of the upper and lower sideband amplitudes and corresponding phase detector outputs. The circled areas show the output during the pulse period. It can be seen that although the signal is quite noisy the phase readings for each pulse are similar, indicating that the response time of the detectors is adequate for the clear weather amplitude levels shown here. A comparison of the phase detector data from the satellite with test set data shows that the noise level has been degraded by the spin effects, however, phase measurements to within 10° can be made for high signal levels. As the signal level drops from

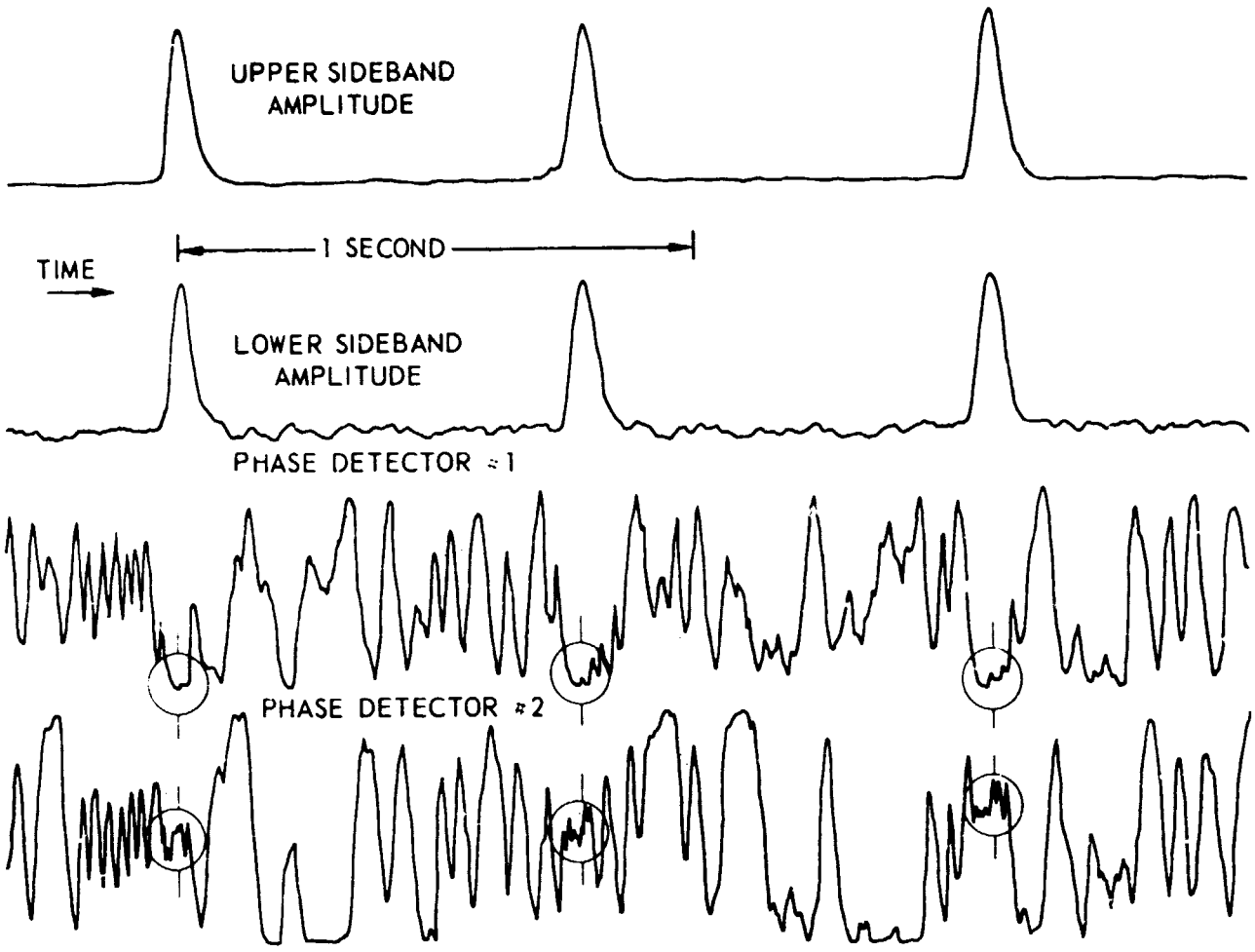

Figure 4.

the maximum value, the phase detector outputs become increasingly noisy and for a 5 db drop become impossible to detect. In comparison, the test set signal will give detectable readings down to 15 db below the maximum expected signal level.

The modifications required on the data reduction program described in Reference 1 because of the satellite spin were significant.

The basic input program change consisted of elimination of the secondly average calculation for the five spin-modulated data channels and instead involves selecting the maximum value of each pulse of amplitude data and the time coincident samples of phase difference.

The original sampling rate for A/D conversion of the five data channels (carrier, USB, LBS amplitudes, phase detector No. 1 and No. 2) was 36 samples per second, or one sample every 28 milliseconds. A non-synchronized sampling of the pulsed data at this rate would result in a serious ambiguity in the data samples, since the 1 db width portion of the signal is only 26 milliseconds in duration.

To overcome this condition, the sampling rate was tripled, to 108 samples per second. The sample values of carrier and upper and lower sideband amplitudes for each second are searched and the maximum value is chosen to represent the signal during that second. Since the sampling occurs every 9.2 milliseconds, one sample will occur within 0.2 db of the peak value of the pulse. If two pulses occur during the one second period of search, two equal maximum values could occur, and the first to occur will be chosen to represent that second.

The phase measurement sampling is done at the same rate, except that the sample time for each secondly period is chosen from the maximum value sample time for carrier amplitude. In order to reduce the effects of the detector output noise three samples are averaged for each one second period, the sample value coincident with the maximum carrier amplitude value, and the sample on either side of that value.

The significant effect of the satellite spin on the analysis of the propagation data is the elimination of a continuous record of amplitude and phase measurements. Signal variations which occur at rates greater than about 0.5 Hz are not detectable because of the spin-modulated data format. The special purpose data correlators designed and built for use on short-term channel fluctuations cannot be utilized with pulsed data.[1]

Long-term fading, fade rates, fade duration, probability densities and distributions are not effected by the spin-condition, and all of the planned computer-generated printouts are available for analysis.

Other special tests, such as site diversity measurements, radiometric and radar correlations, etc., are not impeded by the spin condition, except that fluctuations of the satellite signals at rates greater than about 0.5 Hz cannot be detected, hence, detailed scintillation studies are not available.

Seven stations commenced downlink operations in late September 1969 and the uplink was first utilized in December 1969. Total operational hours for the ATS-V Millimeter Wave Experiment through September 1, 1970 are: main transmitter, 1805 hours, back-up transmitter 304 hours, and uplink 127 hours.

1.3 Rosman Station Configuration

The NASA station, located near Rosman, North Carolina utilizes a dual frequency feed system to permit simultaneous operation of both the uplink and the downlink with a 15 foot Cassegrain antenna system. The feed system consists of a fin (or pin) loaded aperture which allows independent beam shaping at the 15.3 and 31.65 GHz frequencies.

The antenna system includes a program-autotrack capability for continuous satellite tracking. The spin condition of the ATS-V satellite prevents the utilization of the conical scan autotrack system, but program track has functioned adequately with updates generated from the satellite orbital parameters.

Figure 5 shows the Rosman station with the main 15 foot antenna system, equipment trailer, and radiometer and radar pedestals.

The Rosman station includes the following supporting meteorological measurements:

1. Integrated on-beam radar returns and RHI presentations.
2. Radiometer temperature, on-beam, at Ka and Ku-bands.
3. The outputs of 10 tipping rain buckets, placed under the beam.
4. Wind Speed
5. Wind Direction
6. Ambient Temperature
7. Dew Point Temperature
8. Atmospheric Pressure
9. Cloud Cover Photos
10. Weather Class

Figure 6 shows the NASA Rosman station block diagram for recording the propagation and meteorological data. All major data is recorded on the 14 channel magnetic tape and on strip charts for back-up. In addition a number of status functions are recorded on the tape to provide information for the data reduction program.

Following the recording process, data tapes are mailed on a weekly basis to the Goddard Space Flight Center for data reduction and processing. At this point the analog tape contents are digitized and re-recorded on digital magnetic tape.

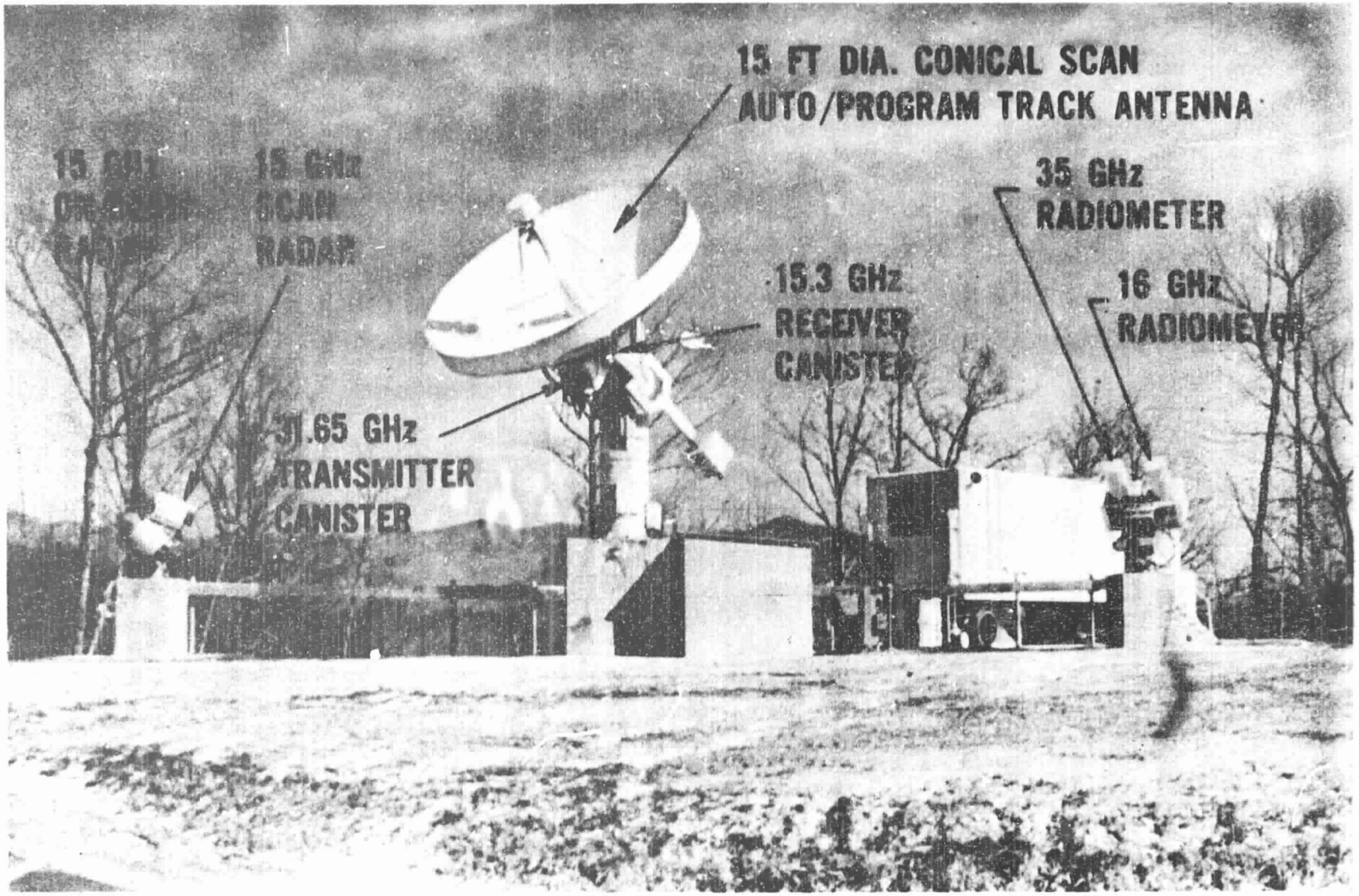

Figure 5. NASA Rosman, North Carolina Station

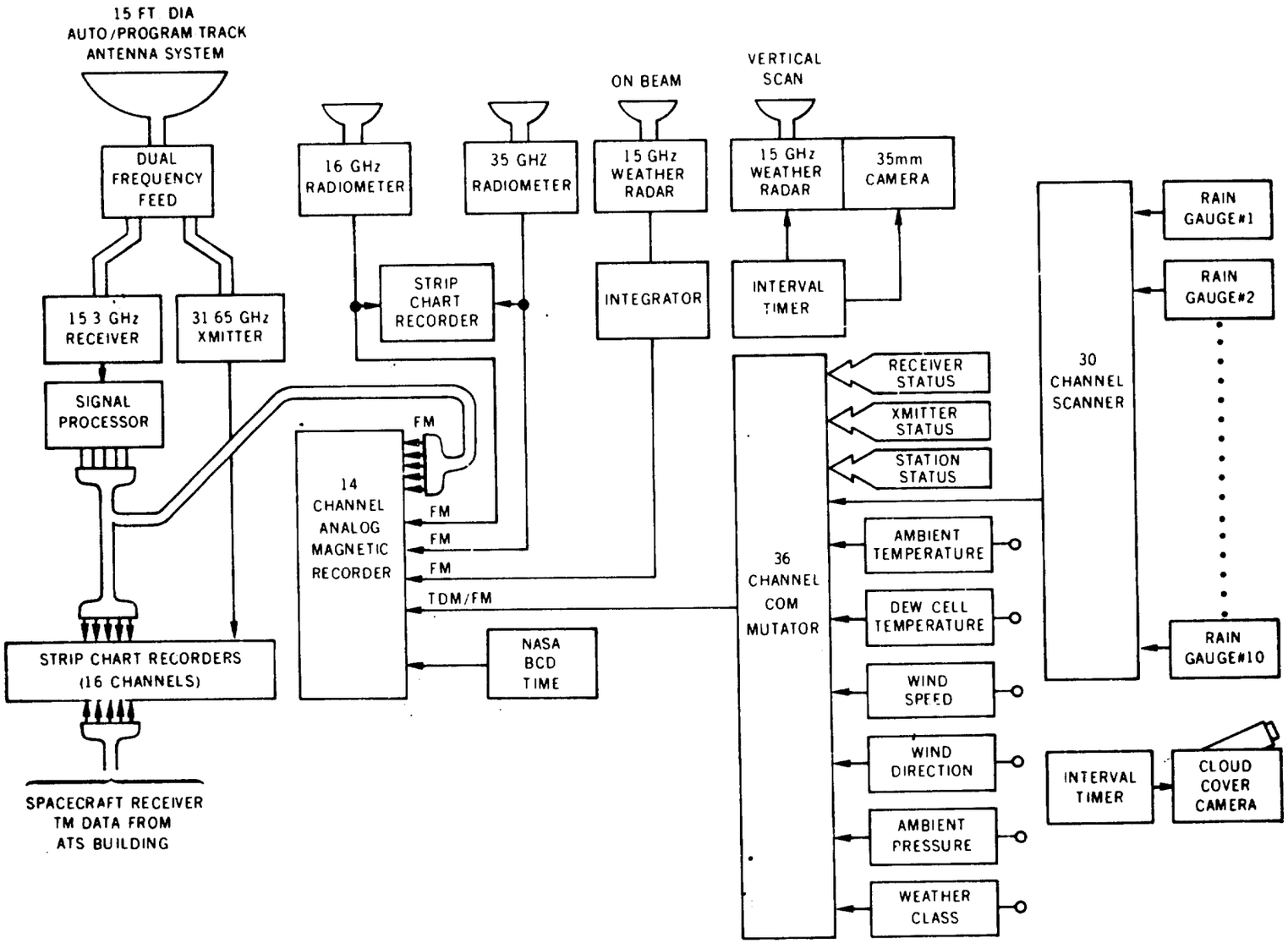

Figure 6. The NASA Rosman, North Carolina, Millimeter Wave Station

The 15.3 GHz ground receiver is similar in design to the 31.65 GHz spacecraft receiver, but some improvements have been possible due to the lower RF frequency and because the ground system is not power and weight limited as is the spacecraft equipment.

A significant difference is the inclusion of an RF amplifier at 15.3 GHz resulting in a front end signal sideband noise figure of 7 db (max.). The RF amplifier is a single stage TDA employing a GASb tunnel diode with a gain of 17 db and a 3 db bandwidth of 600 MHz. The temperature of the amplifier is stabilized at 65°C with a proportionally controlled heater. Some of the major receiver performance characteristics are listed below:

Frequency Stability: ±1 part in 10^8 per 0.1 sec (max.)
±3 PPM per year

PLL Search Range: ±300 kHz

Minimum Sensitivity (Hold-in Threshold): -145 dbm

Amplitude Measurement Range: 32 db

Absolute Amplitude Measurement Error: ±1 db max.

Phase Measurement Error: ±2.5° at maximum signal level.
1° per db down to 20 db below max. signal level.

A complete calibration and test set provides test signals to calibrate amplitude and phase in all modes of operation over the full range of expected levels.

The uplink transmitter for the ATS-V Millimeter Wave Experiment, built by the Hughes Research Laboratories (HRL), consists of a 31.65 GHz klystron signal source, a varactor upconverter modulator, and a traveling wave tube (TWT) power amplifier system. The overall block diagram of the transmitter is shown in Figure 7. The 31.65 GHz frequency stabilized output of the klystron is delivered to a varactor frequency upconverter which is capable of AM, FM, or PM modulation with bandwidths of hundreds of megahertz. The sideband programmer provides automatic or manual selection of 1 MHz, 10 MHz, or 50 MHz sidebands for the transmitted signal.

The stabilized klystron output is directed through a waveguide switch to either the modulation mode (path 2) or high power CW mode (path 1). In the modulation mode, the signal is fed through a ferrite circulator to the upconverter where the

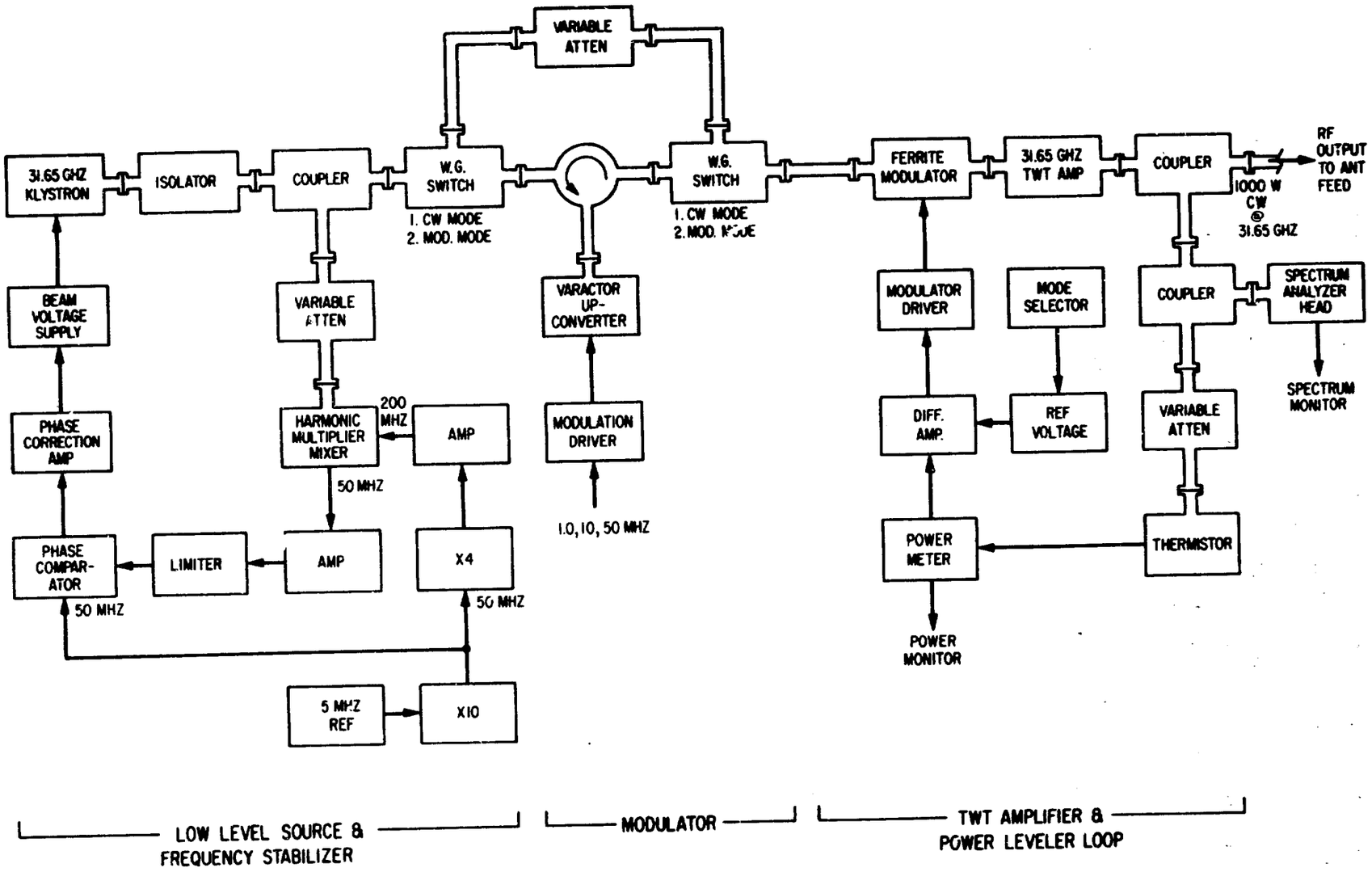
31.65 GHZ KLYSTRON
ISOLATOR
COUPLER
W.G. SWITCH
1. CW MODE
2. MOD. MODE
VARIABLE ATTEN
W.G. SWITCH
1. CW MODE
2. MOD. MODE
FERRITE MODULATOR
31.65 GHZ TWT AMP
COUPLER
RF OUTPUT TO ANT FEED
1000 W CW @ 31.65 GHZ
BEAM VOLTAGE SUPPLY
VARIABLE ATTEN
VARACTOR UP-CONVERTER
MODULATOR DRIVER
MODE SELECTOR
COUPLER
SPECTRUM ANALYZER HEAD
SPECTRUM MONITOR
PHASE CORRECTION AMP
HARMONIC MULTIPLIER MIXER
200 MHZ
AMP
MODULATION DRIVER
DIFF. AMP.
REF VOLTAGE
VARIABLE ATTEN
50 MHZ
1.0,10, 50 MHZ
PHASE COMPAR-ATOR
LIMITER
AMP
X4
50 MHZ
50 MHZ
POWER METER
THERMISTOR
POWER MONITOR
5 MHZ REF
X10
LOW LEVEL SOURCE & FREQUENCY STABILIZER
MODULATOR
TWT AMPLIFIER & POWER LEVELER LOOP

Figure 7.

sideband modulation is produced. In the high power CW mode, the signal is fed through a variable attenuator directly to the output port to the power amplifier.

The TWT is a coupled cavity structure with a 450 MHz 3 db bandwidth. It has a saturated output power of over 1000 watts (CW) but is normally operated at 100 watts during clear weather conditions. The higher power capability provides an additional margin for CW propagation measurements through deep fades.

The measured fade margins available at 15.3 GHz are 15 db with the main transmitter, and 24 db with the back-up transmitter. The reduced margin with the main transmitter is due to a 9 db power degradation which occurred in February 1969. The signal has remained stable since then, and no further degradations have been observed. The full prelaunch power (250 MW) is available on the back-up transmitter for periods of up to 2 hours in duration. Both transmitters are available on call by the participating stations on a 24 hour per day, 7 day per week basis.

The measured uplink fade margin is 30 db with the transmitter in the CW mode.

2.0 PROPAGATION MEASUREMENTS

This section presents a summary of a number of high precipitation events recorded at Rosman with both the downlink and uplink. Later sections will cover attenuation statistics and compare measured attenuation with predictions from ground measured rainfall rate, sky temperature, and radar backscatter.

The time plots of 15.3 GHz downlink carrier attenuation, 16 GHz sky temperature, 15.6 GHz radar backscatter, and three rainfall rates are shown for five weather events in Figures 8 through 12. This section will discuss the general characteristics of the time plots. Details of the measurement techniques and analyses will be discussed in later sections.

The carrier attenuation is referenced to the measured clear weather level at the Rosman station (0 db). The values given are corrected to ±.5 db for transmitted power variations, daily spacecraft movement, and receiver calibration changes. Periods of manual antenna adjustment are shown on two of the plots by "connected arrows," and signal variations during these periods should be disregarded. The antenna system was in a program track mode during the other runs and manual adjustment was not required.

For day 92, two fades of 13.9 db and 10.3 db were observed, and the sky temperature tracked quite well. The radar peaked about 4 minutes before the first fade, and about 3 minutes before the second. (The jumps of backscatter level on the time plot during the first peak are gain step changes made to keep the

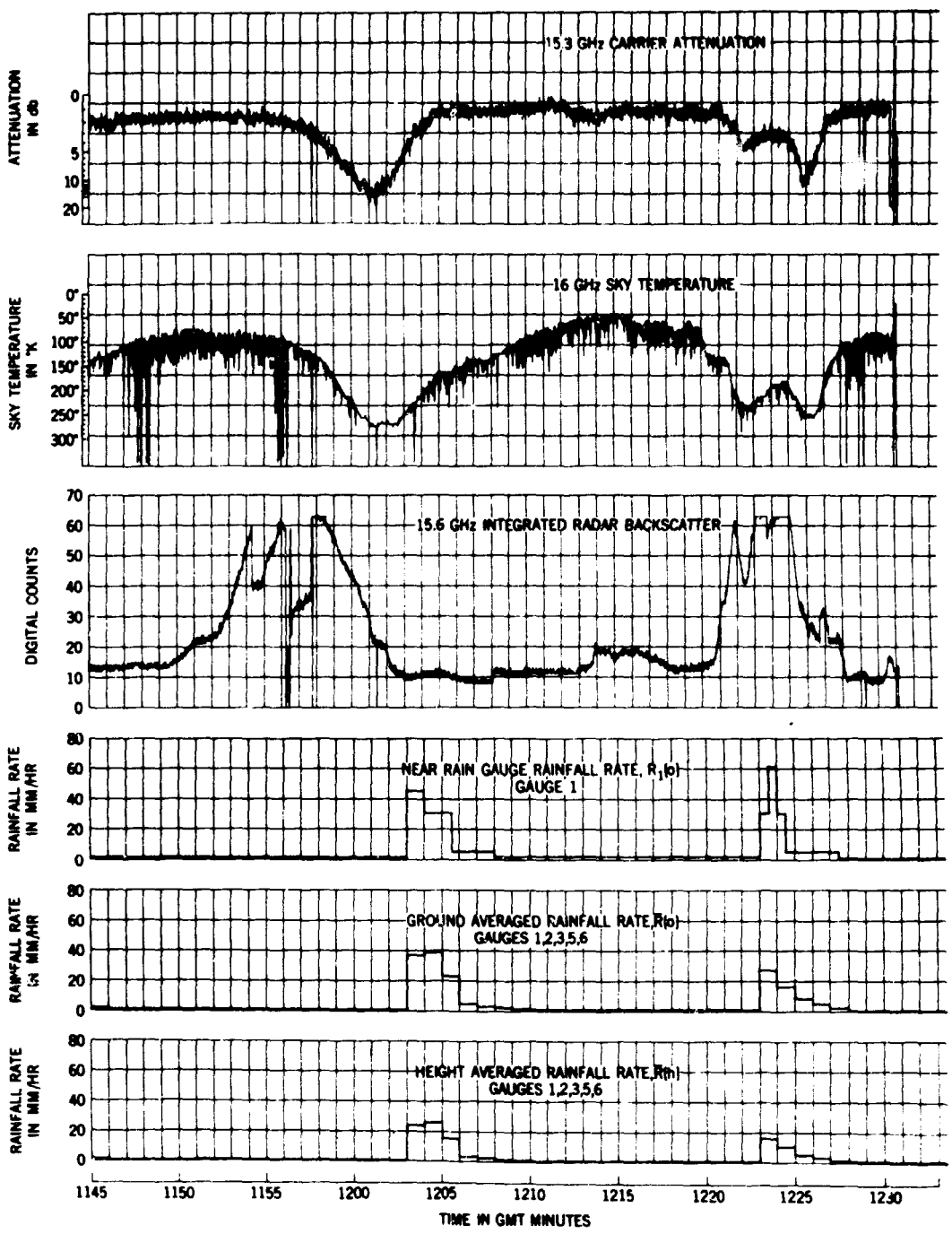

Figure 8. Propagation Measurements During Rainstorm, Rosman, N.C.
Day 92, April 2, 1970, 1145 to 1233 GMT

signal level below 5 volts.) The rainfall rate, however, peaked two minutes after the first fade was observed and about two minutes before the second.

Day 142 consisted of a heavy thunderstorm combined with large hail and moderate winds. The attenuation level reached a maximum of 8.8 db at 2014 GMT and the hail did not noticeably effect the signal, even though it appeared to compromise about 50% of the precipitation during the peak period (2003 to 2009 GMT). The sky temperature again tracked well during the storm reaching a peak of 239°K at 2014 GMT. The radar was not operational.

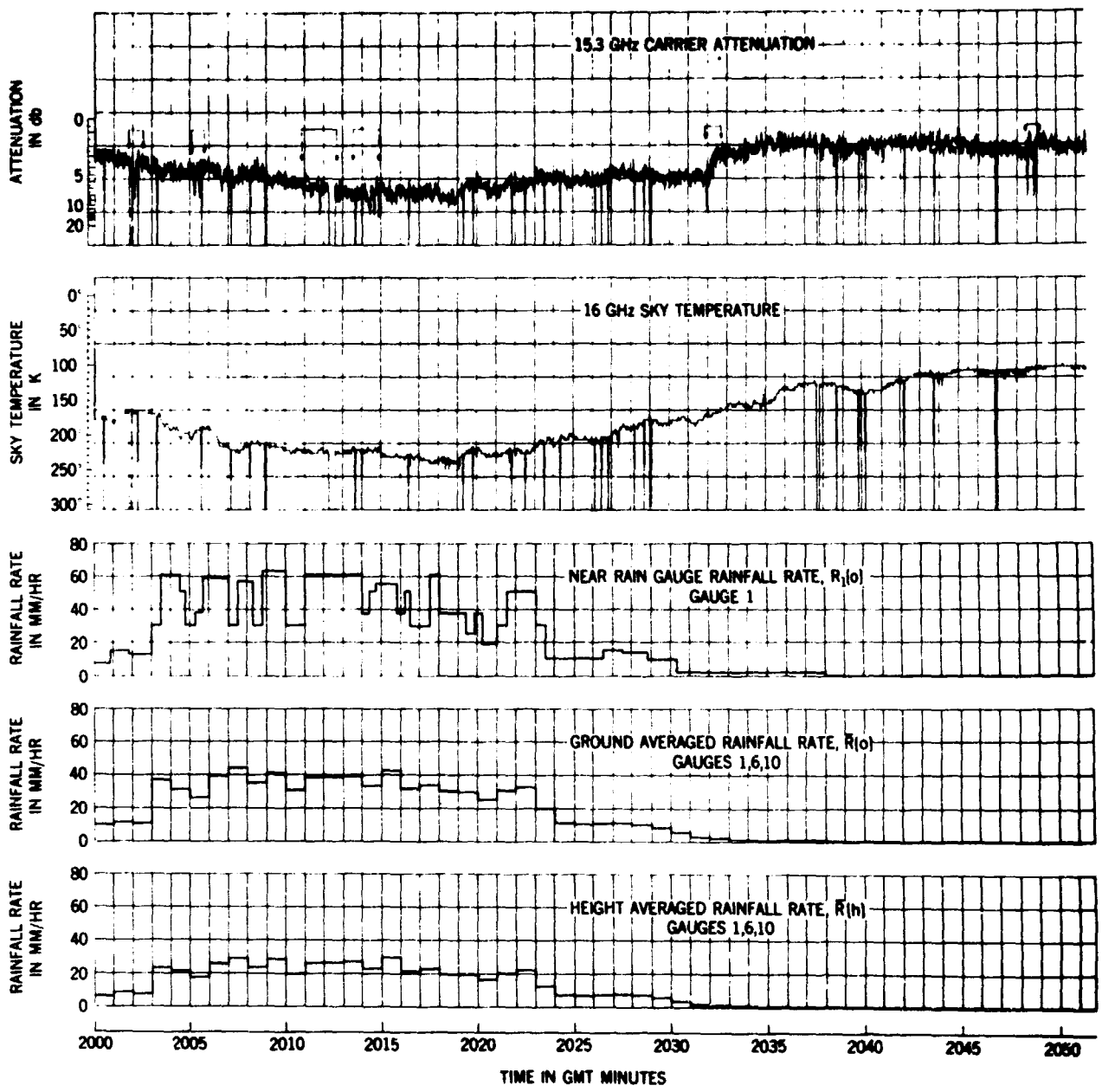

Figure 9. Propagation Measurements During Hailstorm, Rosman, N.C.
Day 142, May 22, 1970, 2000 to 2100 GMT

On day 155 (Figure 10), a moderate rain occurred from 1400 to 1430 GMT which caused the sky temperature to increase but had little effect on the satellite attenuation. A heavy burst of rain commenced at about 1435 GMT, and the signal level dropped 11 db in four minutes until it dropped out at 15 db. The sky temperature also rose sharply and peaked at 260°K for about six minutes.

The back-up transmitter was energized at 144130 GMT, the antenna was peaked, and the signal measured 13 db attenuation at 1445 GMT. The signal level then began to increase and the attenuation was 5 db at 1449 GMT and 2 db at 1500 GMT.

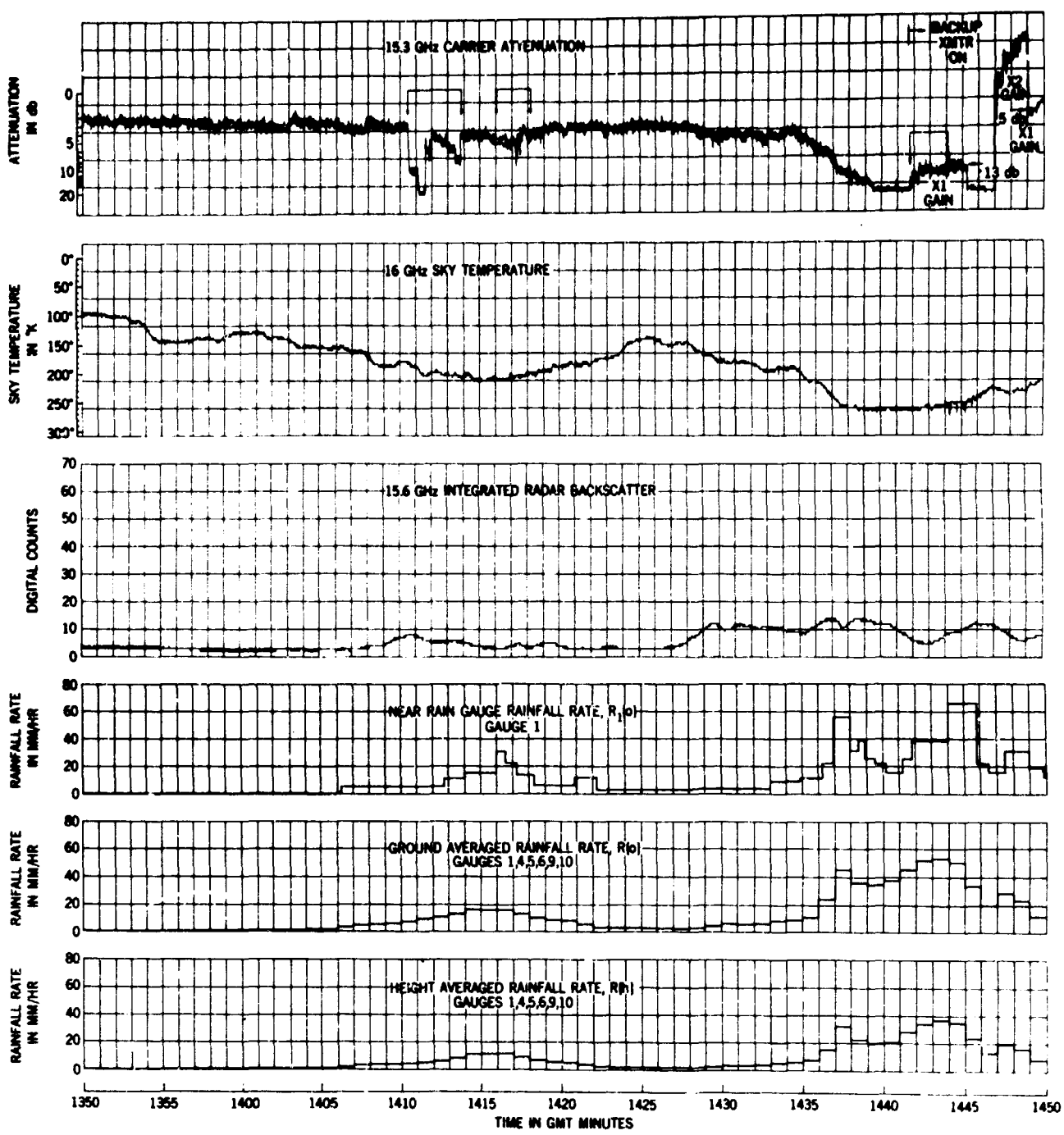

Figure 10. Propagation Measurements During Rainstorm, Rosman, N.C.
Day 155, June 4, 1970, 1350 to 1450 GMT

A second period of rain occurred on day 155 (Figure 11) with a peak of 8 db attenuation at 1711 GMT.

The heaviest rain observed on the downlink to date occurred on day 156 (Figure 12). The signal dropped sharply at 1740 GMT and lock was lost at 174350 GMT. The sky temperature also rose sharply during this period and "peaked out" for about 3 minutes, from 1743 to 1746 GMT. Rain rates as high as 76.2 mm/hr were recorded on the rain gauges during the storms.

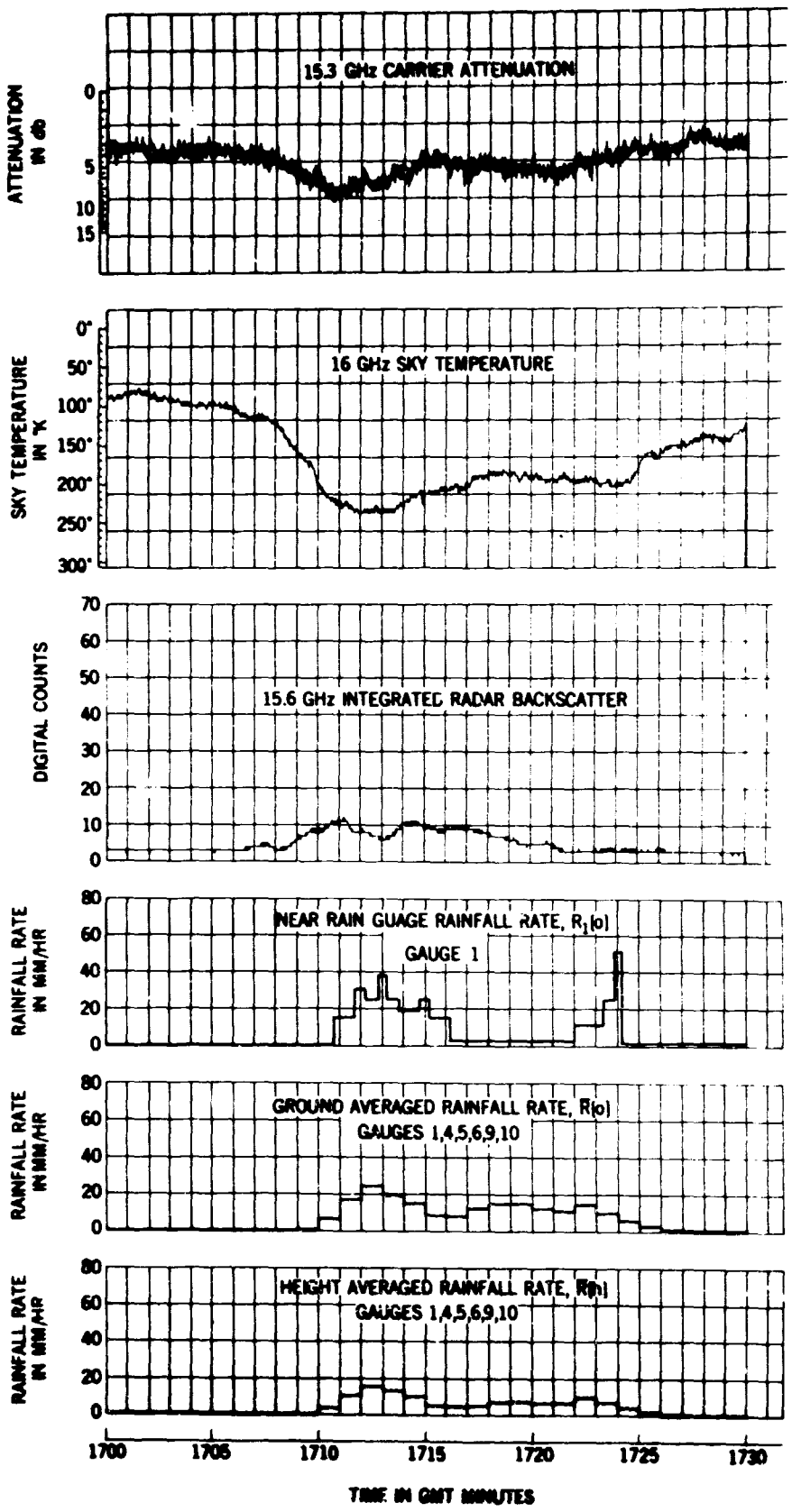

Figure 11. Propagation Measurements During Rainstorm, Rosman, N.C. Day 155, June 4, 1970, 1700 to 1730 GMT

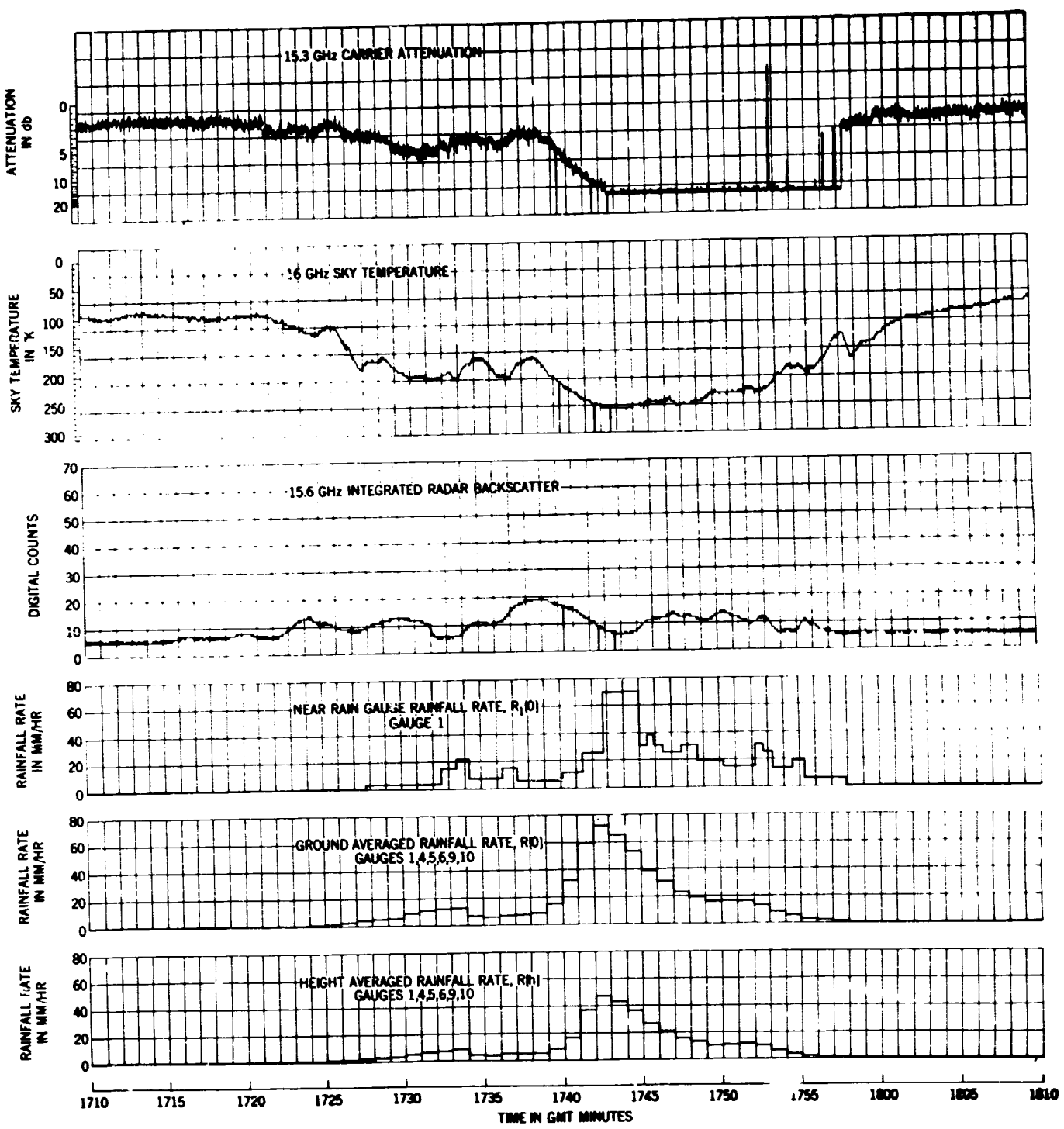

Figure 12. Propagation Measurements During Rainstorm, Rosman, N.C.
Day 156, June 5, 1970, 1710 to 1810 GMT

The radar backscatter did not show good correlation with measured attenuation or rainfall during any of the storm periods presented. A small trend is noticeable on day 155 (Figure 11) and is discussed further in a later section.

Time plots for two uplink periods are shown in Figures 13 and 14. On day 167 a peak attenuation of 18 db occurred at 31.65 GHz. The corresponding 15.3 GHz attenuation was 7.7 db, with rainfall rates as high as 75 mm/hr recorded on the ground.

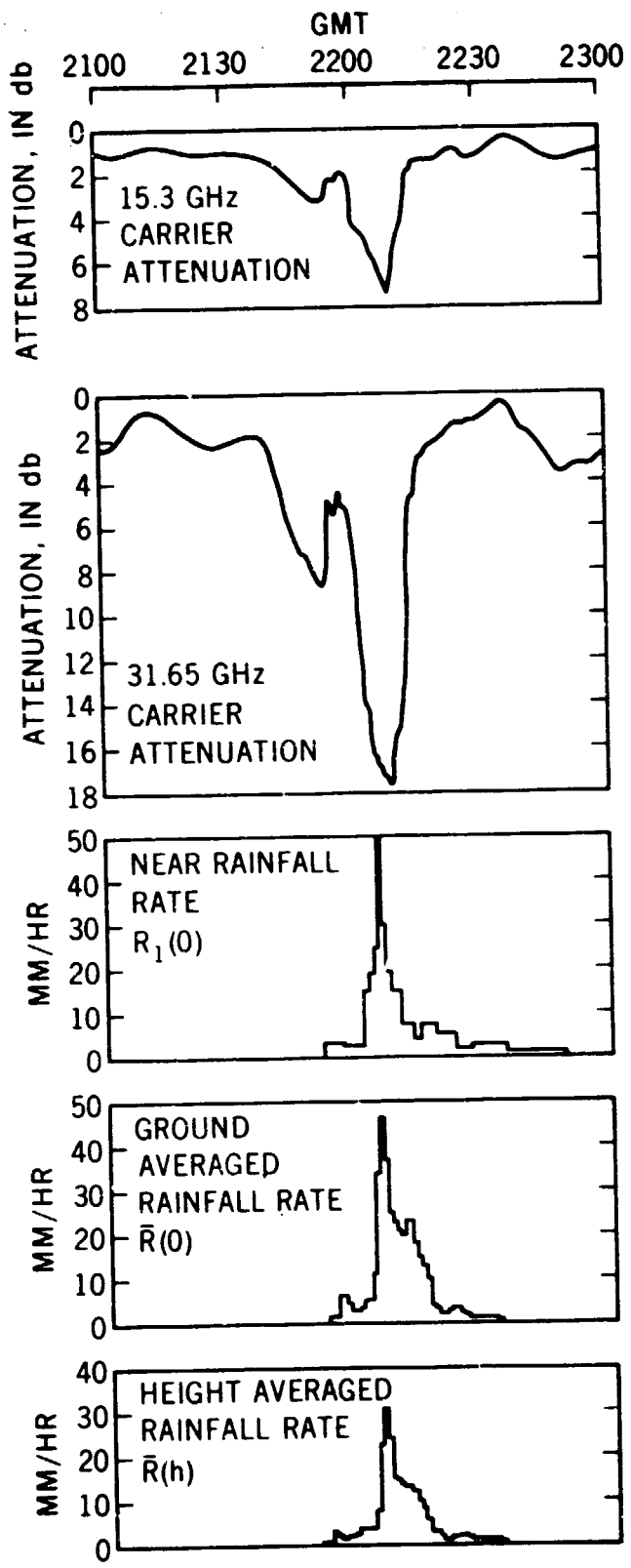

Figure 13. Uplink-Downlink Attenuation During Rainstorm Day 167 June 16, 1970 2100 to 2300 GMT WC-7 (Continuous Rain)

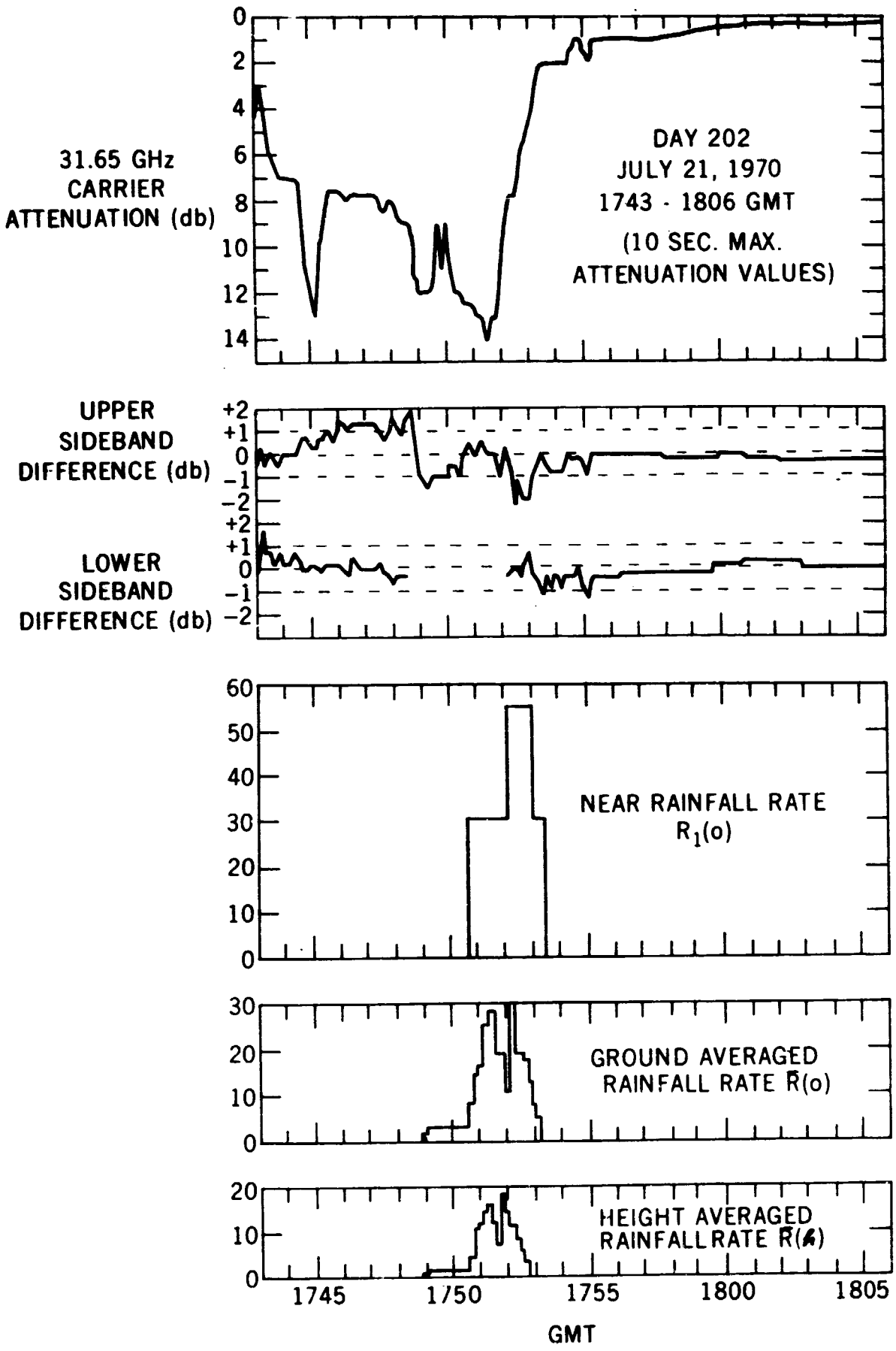

Figure 14. Uplink 50 MHz Sideband Variations During Rainstorm

The time plot for day 202 (Figure 14) shows a prolonged fade which lasted for 11 minutes with three peaks of 13 db, 12 db, and 14 db. Also shown on the figure is the difference in db, between the carrier and the 50 MHz sideband amplitudes during the storm. The variations are within the total link measurement accuracy for the major portion of the run.

The first peak of attenuation occurred with no rainfall recorded on the ground. The last two peaks of attenuation correspond to the two peaks observed on the ground and height averaged rainfall rates, which are discussed further in the next section.

2.1 Attenuation and Rainfall Rate

The rainfall rate, or rain intensity, as monitored by ground located rain gauges is the most popular measurement available in propagation studies, in part because of the ease of making the measurement and also because of the extent of rain statistics available from weather bureau records. Good correlations of attenuation with rain gauge measurements have been demonstrated for terrestrial millimeter wave links (References 8, 9, 10, 11 among many others), but extension to earth-satellite links has yet to be demonstrated.

The attenuation of millimeter wave energy due to rain is dependent on drop size distribution and rain intensity. Gunn and East (Reference 12) proposed the use of an empirical expression of the form

$$A = a R^b \tag{1}$$

to relate the attenuation to the rainfall rate. A is the attenuation in db/km and R is the rainfall rate in mm/hr. The parameters a and b are frequency dependent constants.

A number of authors have developed values of the parameters a and b based on theoretical and experimental data at a number of frequencies. The initial values of a and b utilized on the ATS-V Experiment were determined by comparing the results available in the literature and selecting representative values for the two frequencies of interest (Reference 3).

The resulting relations are:

$$A\left(\frac{db}{km}\right) = 0.035 R^{1.155} \quad @\ 15.3\ GHz \tag{2}$$

$$A\left(\frac{db}{km}\right) = 0.2R^{1.0} \text{ @ } 31.65 \text{ GHz} \qquad (3)$$

The total path attenuation at 15.3 GHz and 31.65 GHz predicted from the above relations are plotted in Figures 15 and 16 for various path lengths, L. The 3.57 kM and 4.8 Km lengths correspond to the geometric ground and slant-path distances for the rain gauge network at Rosman.

The rain gauge network consists of 10 "tipping-bucket" gauges located on a ground line the azimuth direction of the ATS-V satellite. Figure 17 shows the dimensions of the network.

The near rainfall rate, R_1 (0), is the rate as given by the nearest gauge, located directly in front of the antenna.

The ground average rainfall rate, $\bar{R}$ (0), is

$$\bar{R}(0) = \sum_{n=1}^{N} \frac{R_n(0)}{N} \qquad (4)$$

where N is the number of buckets in valid operation at the time of measurement and R_n (0) is the reading of the n'th bucket, in mm/hr.

The height average rainfall rate, $\bar{R}$ (h), is

$$\bar{R}(h) = \frac{1}{10} \sum_{n=1}^{10} \left(1 - \frac{h_n}{H} R_n\right)(0) \qquad (5)$$

where h_n and H are defined in Figure 17.

The rainfall rates R_n (0), in mm/hr, are determined by dividing the water accumulated per tip (0.254 mm) by the time (in hours) between adjacent tips. This results in rain rate values which increase in resolution as the rate increases, and gives essentially instantaneous readings for rates above 20 mm/hr.

A direct second by second or minute by minute comparison of measured attenuation with predicted attenuation would yield very little useful data, as seen from the time plots (Figures 8 through 14). Rain rate variations often do not occur in time coincidence with the attenuation increases.

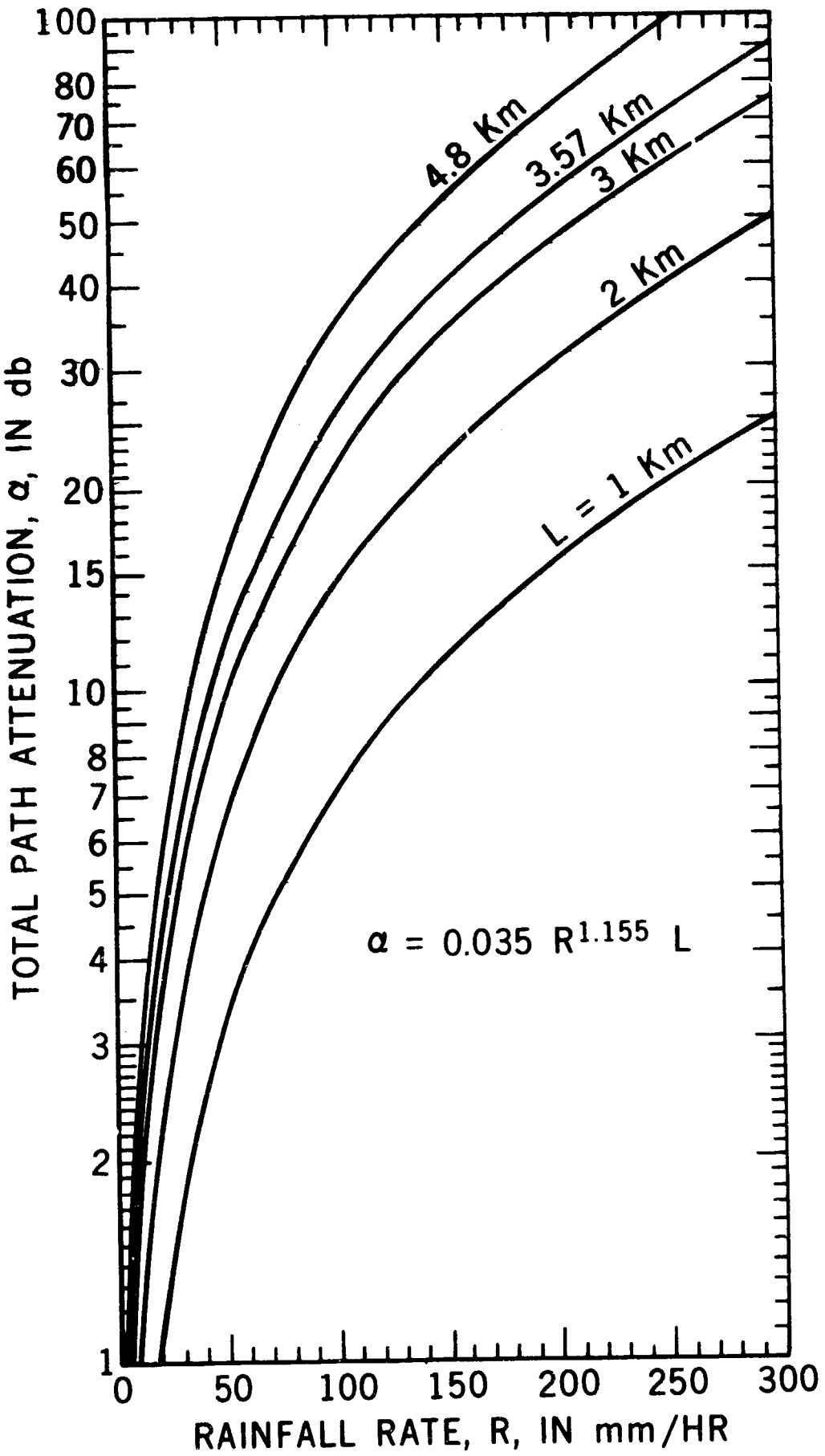

Figure 15. 15.3 GHz Total Path Attenuation Predicted from Rainfall Rate

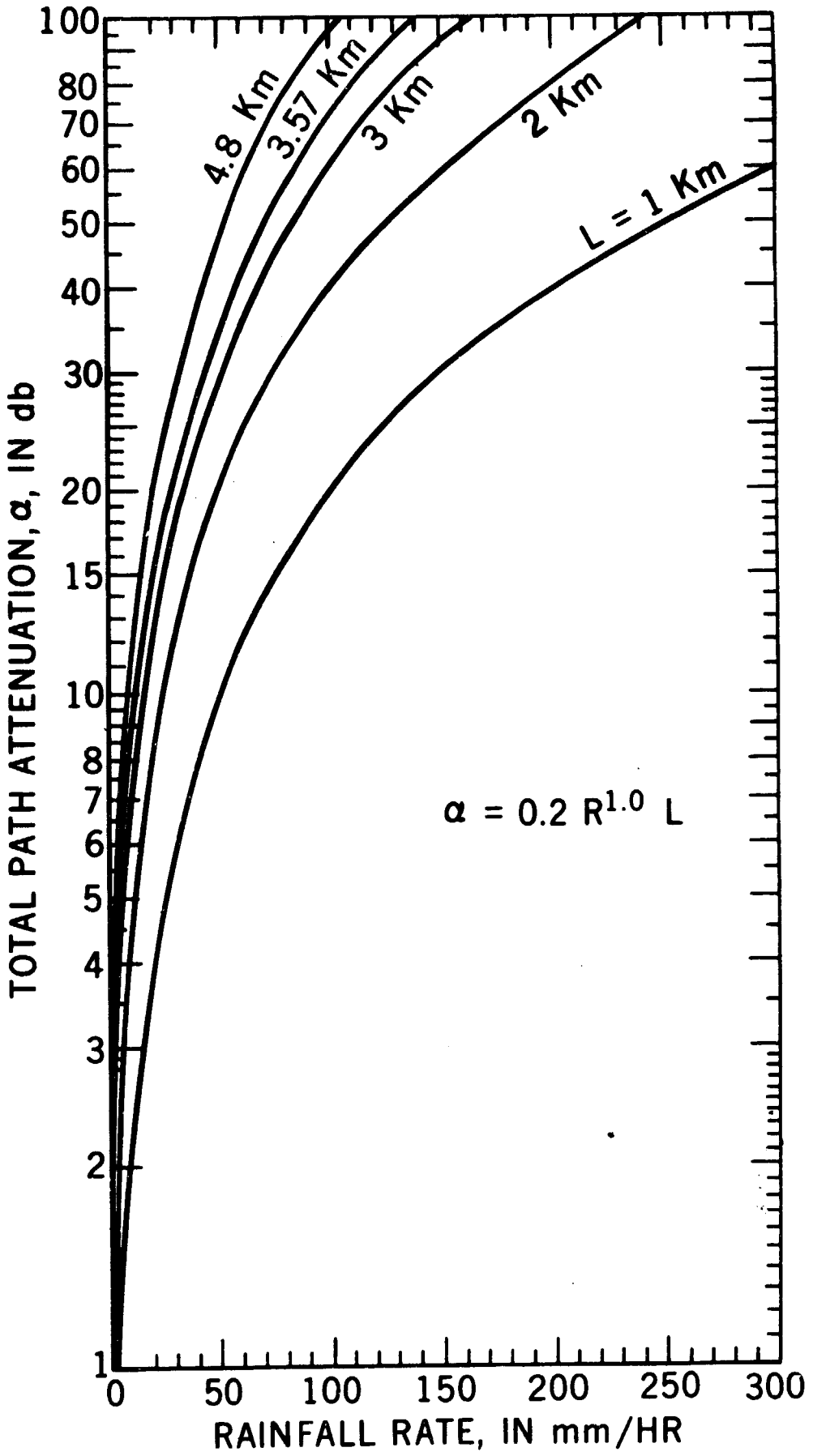

Figure 16. 31.65GHz Total Path Attenuation Predicted from Rainfall Rate

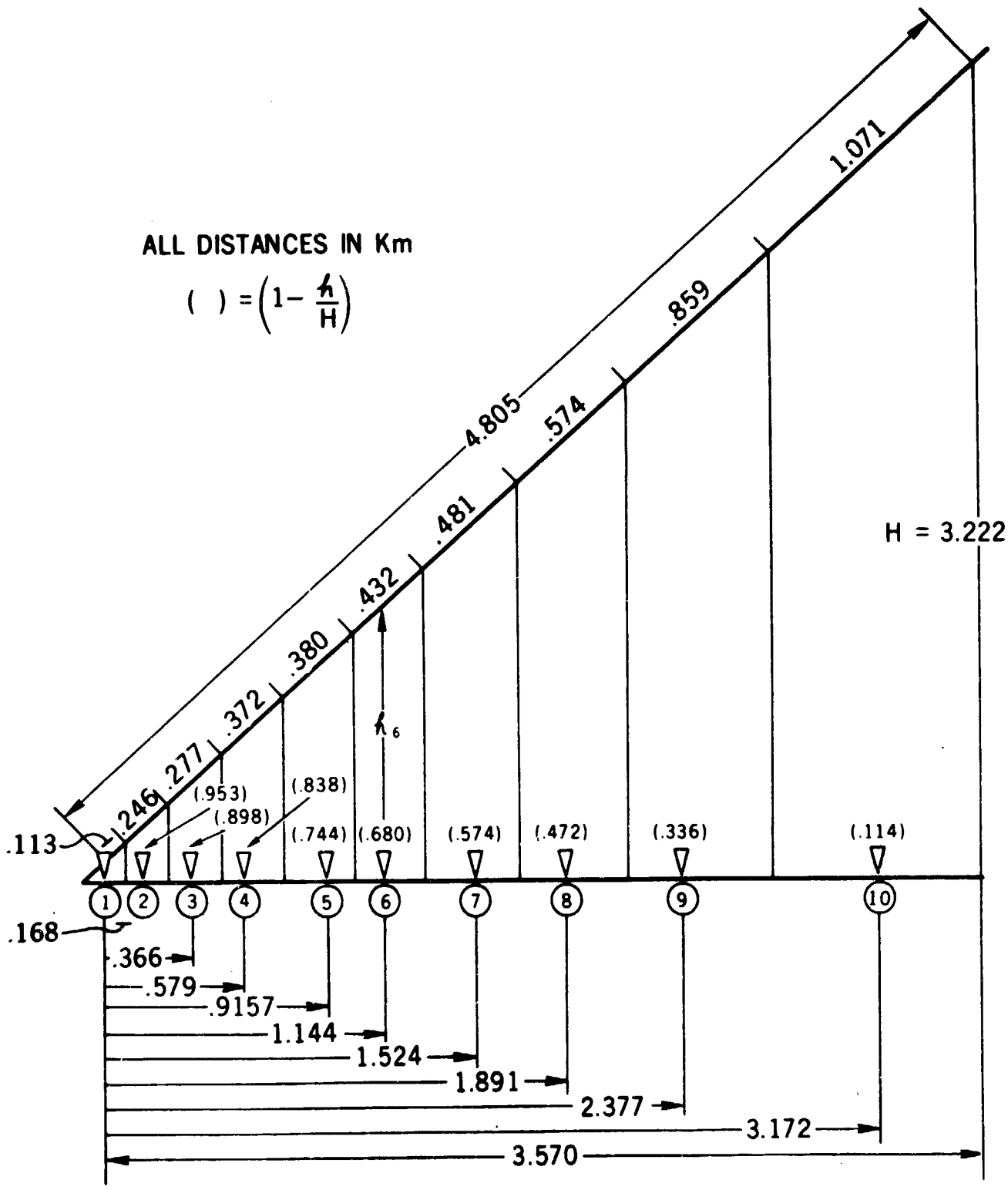

Figure 17. Rain Gauge Network at Rosman, North Carolina Millimeter Wave Terminal

A more meaningful approach is to compare distinct "peaks" of attenuation with corresponding peaks of rainfall rate which occur near the time of occurrence of the attenuation peak. For example, on day 92, the 13.9 db attenuation peak at 1201 GMT is compared with the 45 mm/hr peak for R_1 (0) at 1203 GMT, the 39 mm/hr peak for $\bar{R}$ (0) at 1204 GMT, and the 28 mm/hr peak for $\bar{R}$(h) at 1204 GMT.

The results of peak 15.3 GHz attenuation and peak rainfall rate comparisons for eight storm occurrences are presented in Figure 18. The curves on each plot show the predicted attenuation for the given path length L.

The first interesting characteristic is the reduction in dispersion of the points when averaging techniques are employed. The reduction in dispersion is most pronounced for $\bar{R}$ (h). The best fit prediction curve for $\bar{R}$ (h) is for a slant path of 7.1 km, shown by the dotted line. The corresponding ground length for that slant path is 5.3 Km, shown by the dotted line in the $\bar{R}$ (0) plot. An accurate measurement of an actual "path length" for each storm is difficult, if not impossible to attain, since the definition of what constitutes a true path length is itself a subject for debate.

Similar results occur for 31.65 GHz peak attenuation plots, as shown in Figure 19. For the three storms presented, the prediction curve for $\bar{R}$ (h) with L = 4.8 km, the geometric path length, gives the best fit. The point dispersion is again significantly reduced by height averaging.

2.2 Attenuation and Sky Temperature

The prediction of millimeter wave earth-space attenuation from sky temperature measurements with a small aperture radiometer would be an extremely useful tool in evaluating potential ground station locations for reliability and diversity characteristics. The increased beamwidth resulting from the small aperture radiometer encloses a much larger volume of space than the satellite earth station antenna, however, and this may produce discrepancies between the measured attenuation and that predicted from the sky temperature. The intent of the sky temperature measurements program at Rosman is to compare small aperture sky temperature with measured attenuation and evaluate the prediction characteristics over a large number of storm occurrences.

Two radiometers are in use at Rosman, one at 16 GHz and the second at 35 GHz. Both employ Dicke type systems, with a mechanical modulator at 16 GHz and a ferrite modulator at 35 GHz. The operating characteristics of the radiometers are listed in Table 2. Both antennas are pointed in the satellite direction and have significantly larger beamwidths than the 15 foot antenna system (0.3°).

The prediction of atmospheric attenuation from sky temperature measurements can be accomplished for the case of gaseous absorption with no scattering from the relation

$$T_s = \left(1 - \frac{1}{\alpha_r}\right) T_m \qquad (6)$$

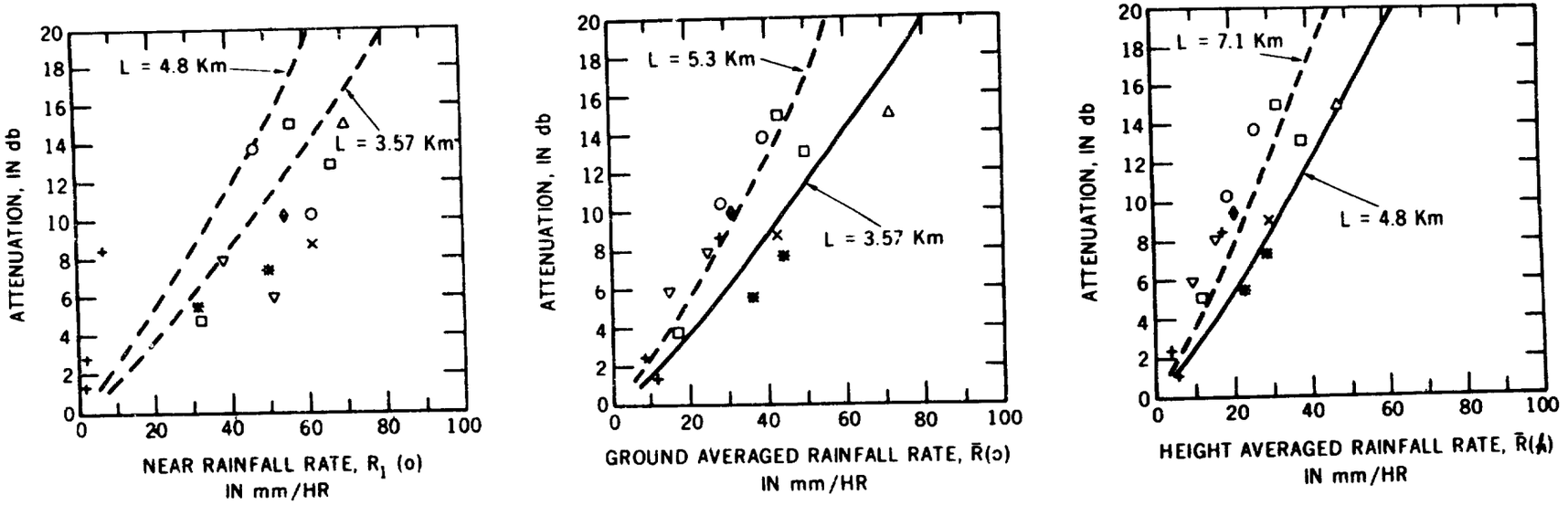

PREDICTED ATTENUATION = $0.035\ R^{1.115} \cdot L$

- o DAY 92, CONTINUOUS RAIN
- × DAY 142, THUNDERSTORM, HAIL
- □ DAY 155, CONTINUOUS RAIN
- ▽ DAY 155, CONTINUOUS RAIN
- △ DAY156, CONTINUOUS RAIN
- ✱ DAY 167, CONTINUOUS RAIN
- ♦ DAY 202, CONTINUOUS RAIN
- \+ DAY 231, CONTINUOUS RAIN

Figure 18. Peak 15.3 GHz Carrier Attenuation vs Peak Rainfall Rate

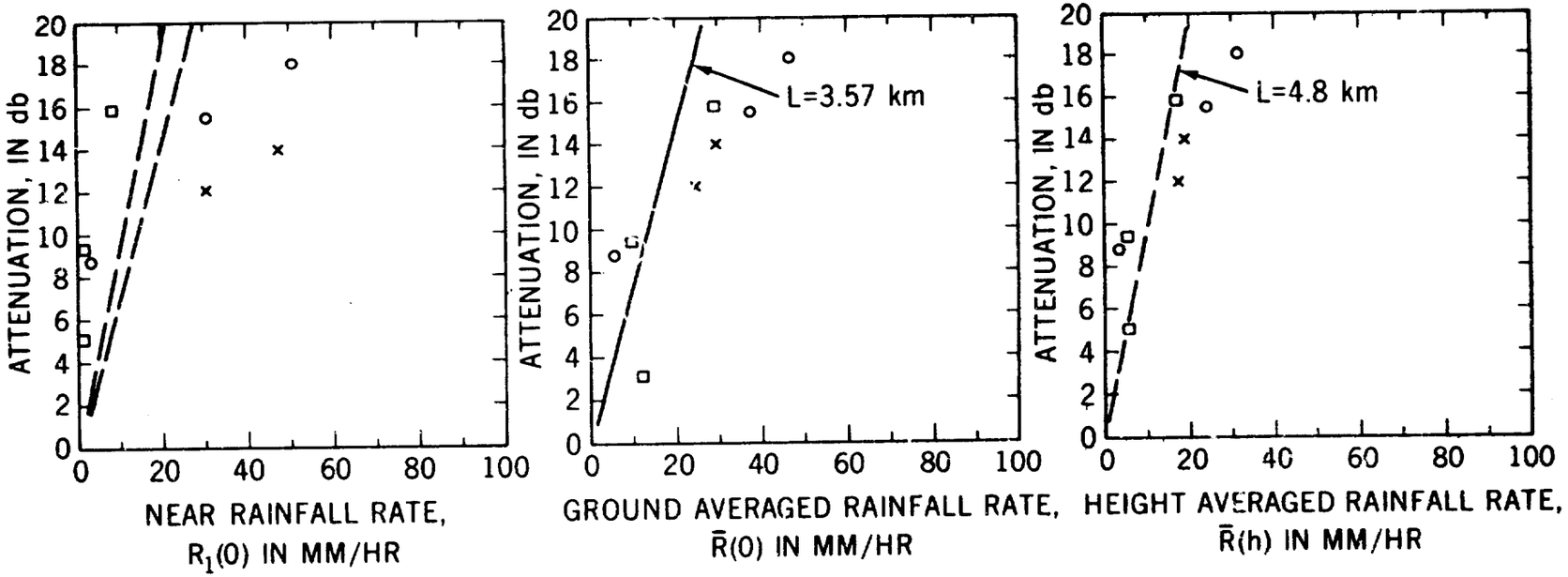

○ DAY 167, CONTINUOUS RAIN
× DAY 202, CONTINUOUS RAIN
□ DAY 231, CONTINUOUS RAIN

PREDICTED ATTENUATION = $0.2\ R^{1.0}L$

Figure 19. Peak 31.65 GHz Carrier Attenuation vs. Peak Rainfall Rate

Table 2
Operating Characteristics for ATS-V Radiometers

Characteristic	16 GHz Radiometer	35 GHz Radiometer
Antenna	TRG Lens Ant.	TRG Lens Ant.
Diameter	12 inch	12 inch
Gain	32 dB	39 dB
Matching (VSWR)	<1.01	<1.01
Antenna efficiency	~0.8	~0.8
Beam width	4.0°	2.0°
RF Amp.	T.D.A. 15 dB (NF7dB)	Not used.
IF Amp.		
Bandwidth	80 MHz	2.0 GHz
Noise Figure	6 dB	12 dB
Local Oscillators	Klystron (Varian)	Klystron (Varian)
Modulator	Mechanical	Ferrite Switching
Mod. Freq.	94 100 Hz	94 100 Hz
Recorder		
Amp. Out	Lock-in Amp 0 - 5V	Lock-in Amp 0 - 5V
Sensitivity $\left(= K \frac{T_{sys}}{\sqrt{B t}}\right)$ (t = 1 sec k = 2	0.22°K	0.45°K
Ambient temp. of radiometer (RF, IF)	40°C ± 1°C	40°C ± 1°C
Hot load	318°K (45°C)	318°K (45°C)
Cold load	Liquid Nitrogen (77°K), dry ice (198°K) or ice cubes (273°K)	

where

T_s = emission temperature of the sky, in °K,

T_m = the mean absorption temperature of the atmosphere in °K,

α_T = atmospheric attenuation factor.

The calculation of attenuation from the above relation is generally limited to clear sky or thin cloud conditions, since the assumptions in the derivation are not valid for appreciable condensed water absorption or scattering in the path.[13]

The mean absorption temperature of the path, T_m, is essentially independent of frequency and is related to the surface temperature, T_g, by

$$T_m = 1.12\, T_g - 50 \tag{7}$$

The atmospheric attenuation, in db, is expressed as

$$\alpha_T\,(\text{db}) = 10 \log_{10} T_m - 10 \log_{10} (T_m - T_s) \tag{8}$$

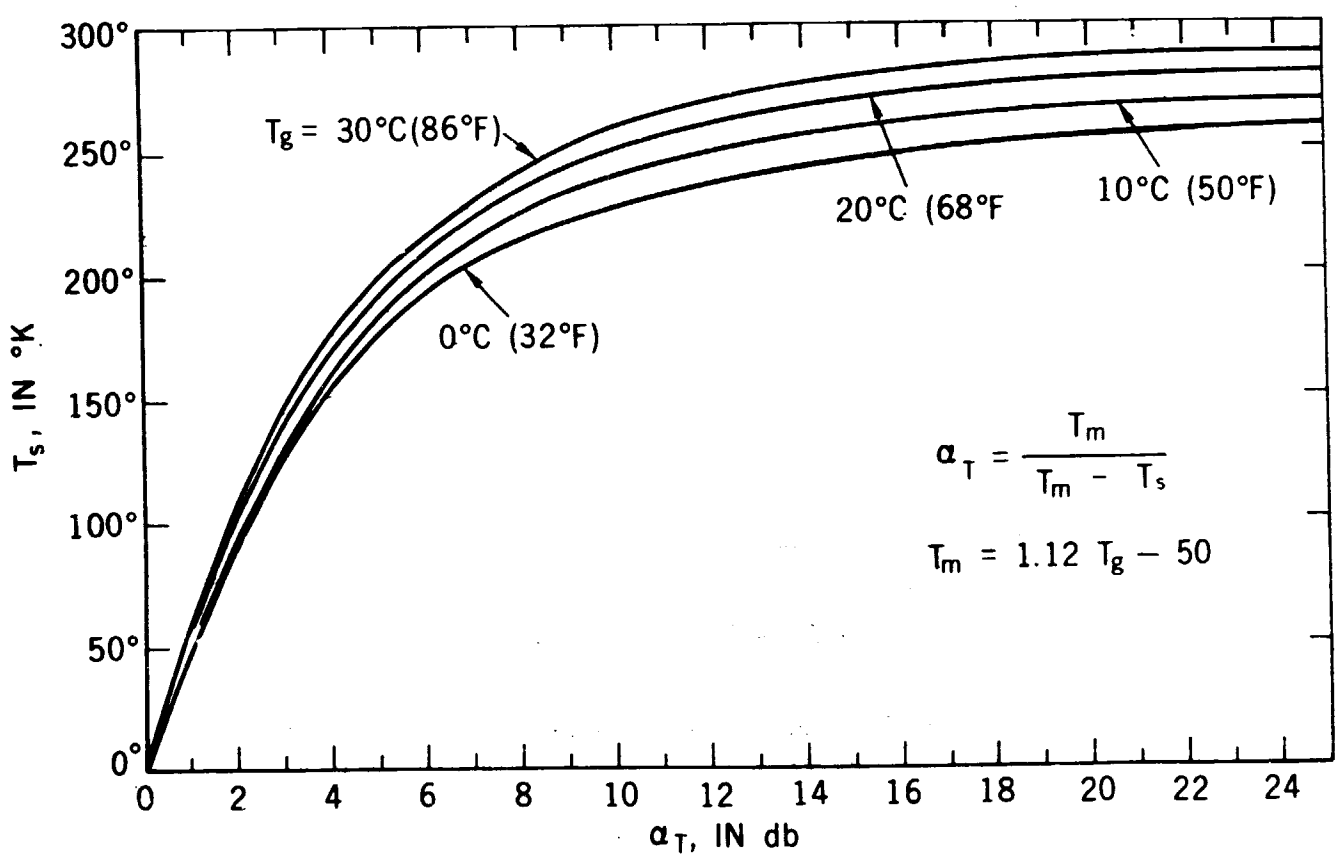

Figure 20. Atmospheric Attenuation Predicted from Sky Temperature

Figure 20 shows α_T (db) as a function of T_s for T_g = 0°, 10°, 20°, and 30°C.

Correlation diagrams of measured 15.3 GHz and 16 GHz sky temperatures for the five storm events previously described in Section 2 are presented in Figures 21 through 25.

The prediction curves on each plot are computed with the average ambient temperature recorded during the storm period, Both attenuation and sky temperature values are based on 30 second averages. The frequency of occurrence of each point is not noted on the diagram, however, most points above 5 db correspond to a single sample, while those below 2 db consist of two or more samples.

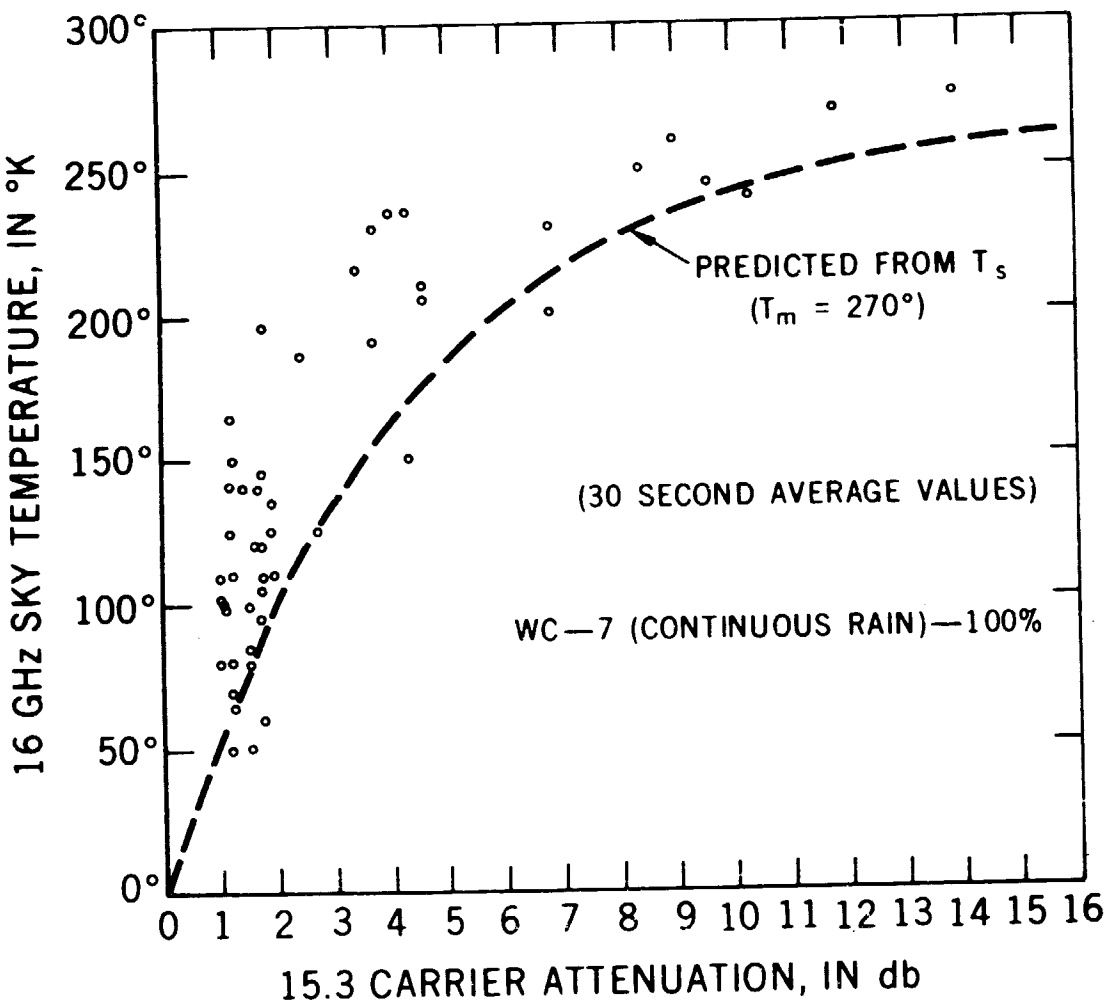

Figure 21. Attenuation-Sky Temperature Correlation Plot
Day 92, April 2, 1970, 1145 to 1230 GMT

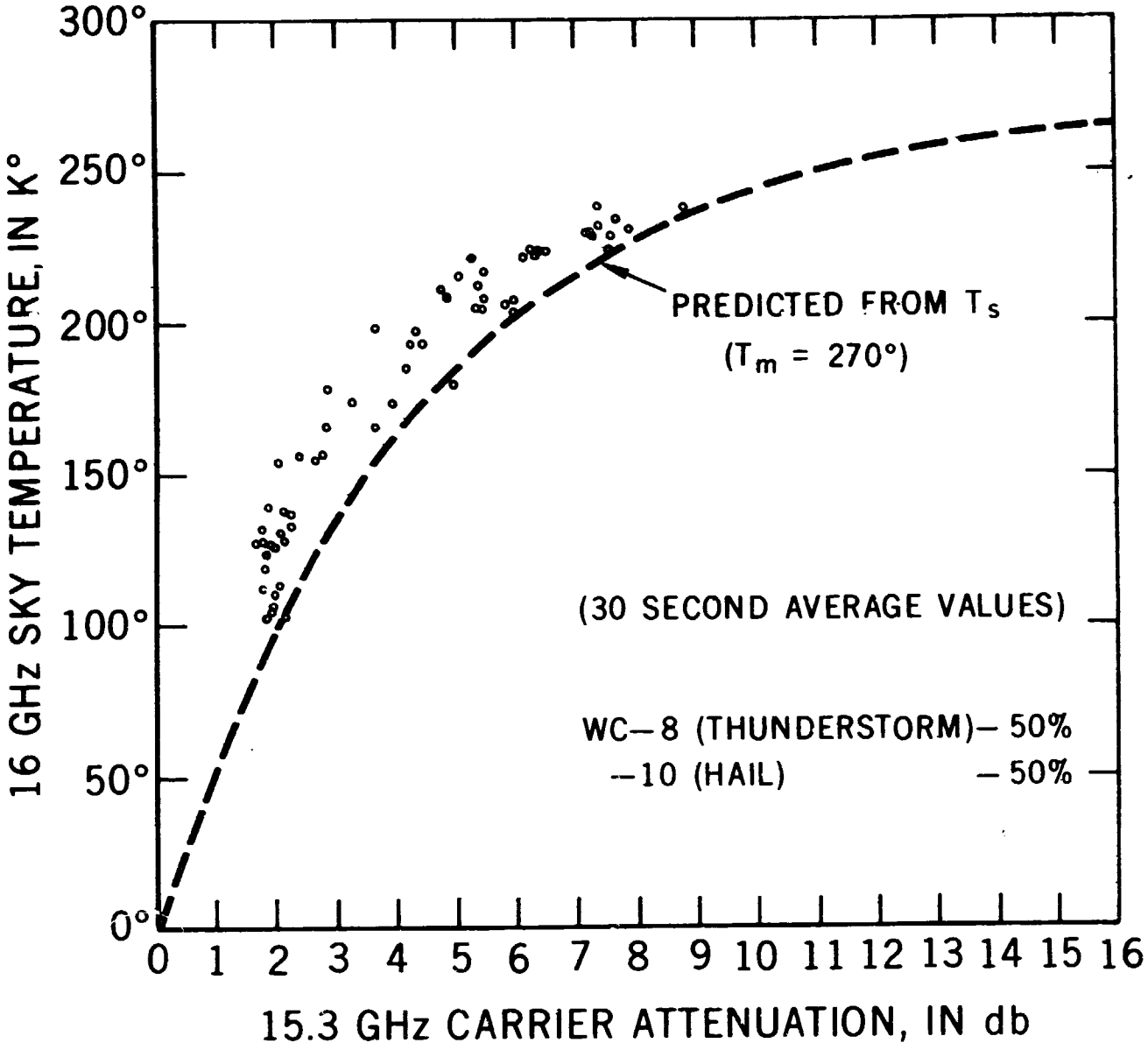

Figure 22. Attenuation-Sky Temperature Correlation Plot
Day 142, May 22, 1970, 2000-2052 GMT

In all cases the major portion of points occurs at or slightly above the prediction curve. On the two days with the highest attenuation, (Figures 23 and 25), the correlation was very good throughout and appears better at the higher levels of attenuation.

Figures 23 and 24 show the variations in correlation within a storm itself. In both samples, which occurred on the same day, the end portion of the run shows better correlation than the leading portion. This effect is most noticeable in Figure 24, where the measured values before 1711 GMT fall far short of the prediction curve.

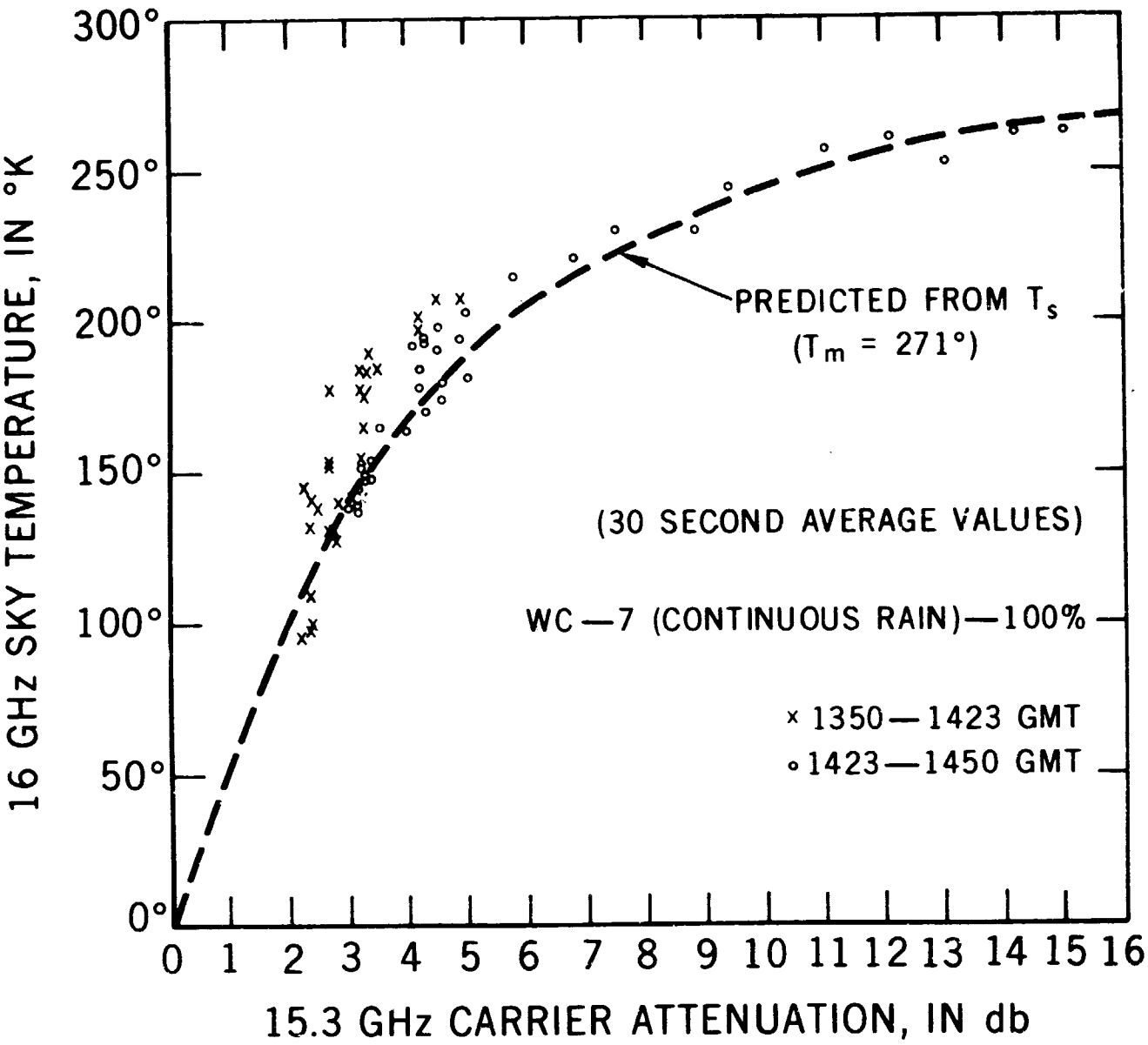

Figure 23. Attenuation-Sky Temperature Correlation Plot
Day 155, June 4, 1970, 1350 to 1450 GMT

Figure 26 shows the cross-covariance coefficient of measured attenuation with predicted attenuation for day 92. This plot produces the rather interesting result that the correlation between sky temperature predicted attenuation and measured attenuation is the highest, (0.81), if one compares the predicted attenuation with the measured attenuation which occurred 30 seconds earlier!

No attempt will be made here to explain this result, or to deduce any conclusion, until data from many more events are available.

Sky temperature comparisons with the 35 GHz radiometer and the 31.65 GHz uplink are under investigation but were not available in time for this report.

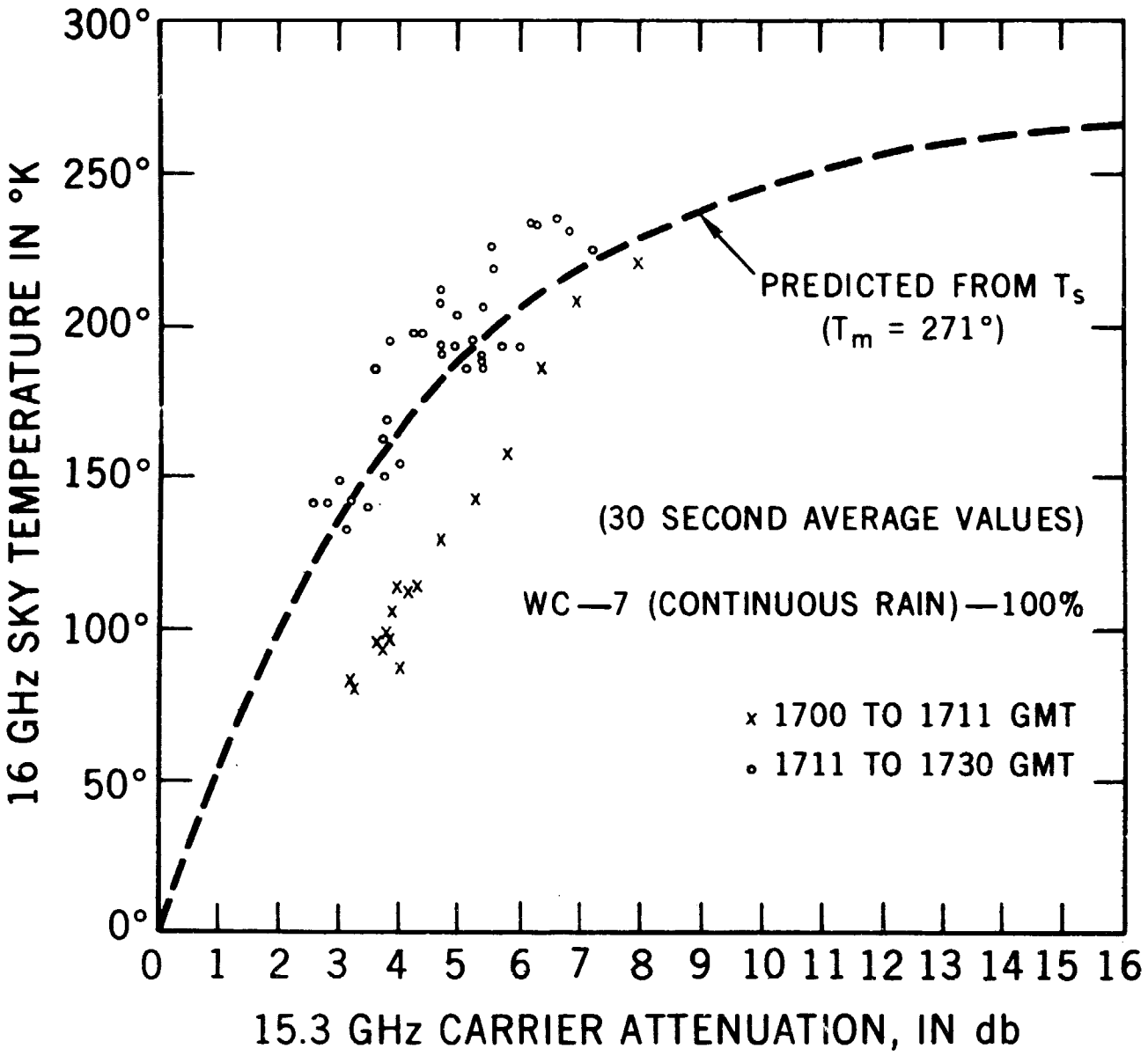

Figure 24. Attenuation-Sky Temperature Correlation Plot
Day 155, June 4, 1970, 1700-1730 GMT

2.3 Uplink and Downlink Comparisons

Comparisons of 15.3 GHz and 31.65 GHz attenuation characteristics simultaneously measured through the same precipitation indicates a wide range of attenuation ratios which vary with each storm, and within the storm itself.

Figures 27 through 30 show the uplink attenuation versus downlink attenuation for four storm events. In the first two examples the attenuation ratio remained fairly constant throughout each storm, at 2:5 to 1 for the first event, and 3.33 to 1 for the second. The last two examples show a wide dispersion of attenuation ratio during the storm. All runs were made during relatively continuous

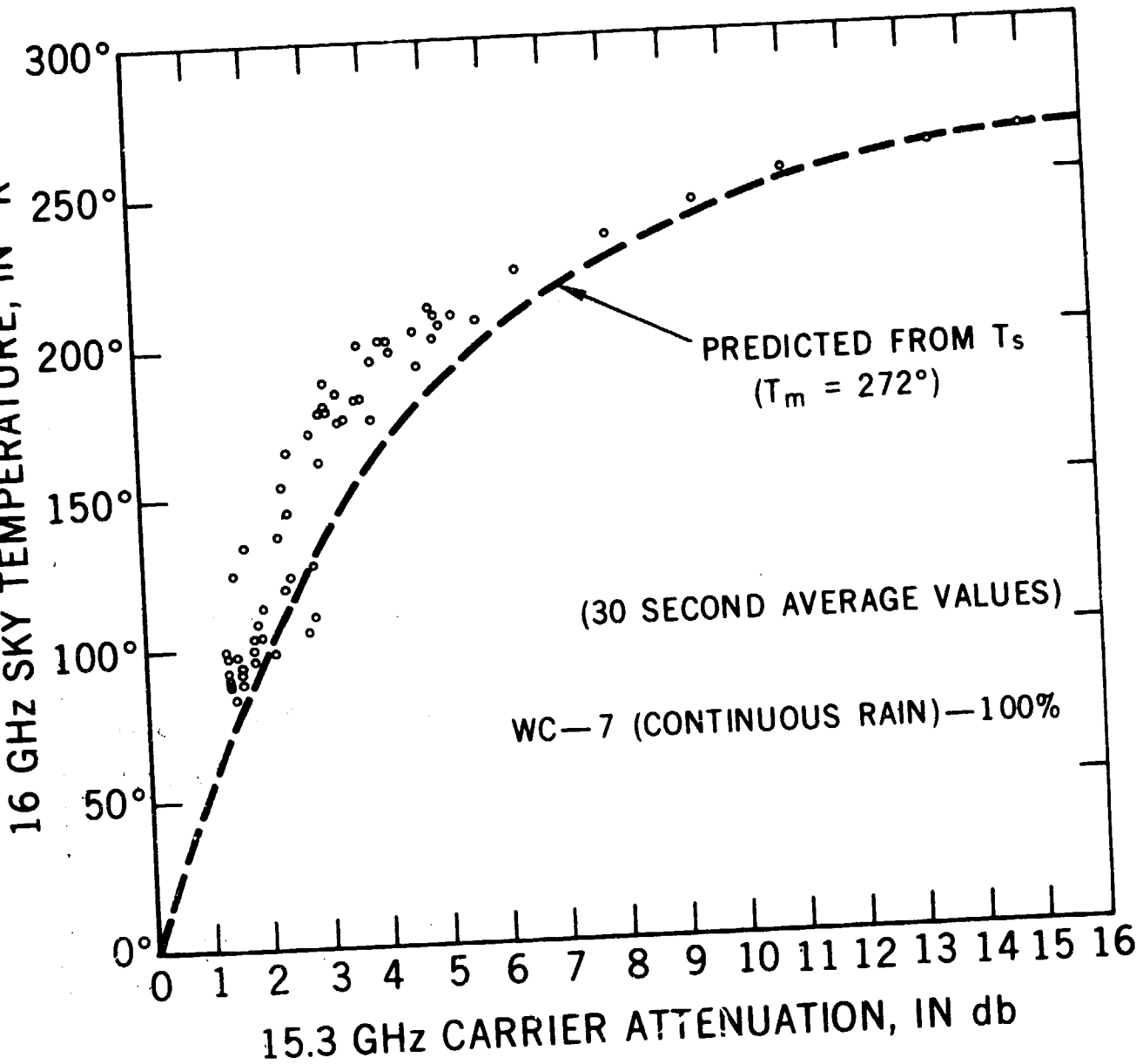

Figure 25. Attenuation-Sky Temperature Correlation Plot
Day 156, June 5, 1970, 1710-1810 GMT

rains with high variations of rain rate occurring for the first two where the ratio was relatively stable.

Variations in drop size distribution will cause a change in the attenuation ratio, and the prediction of attenuation at one frequency based on measurements at another is made difficult by the distribution variations during a storm. An estimate of the drop size distribution may be available, however, for those storms where the ratio remains fairly stable throughout.

Cumulative distributions of uplink and downlink attenuation for days 167, 202, and 231 are shown in Figures 31 through 33. Note that days 162 and 231, which

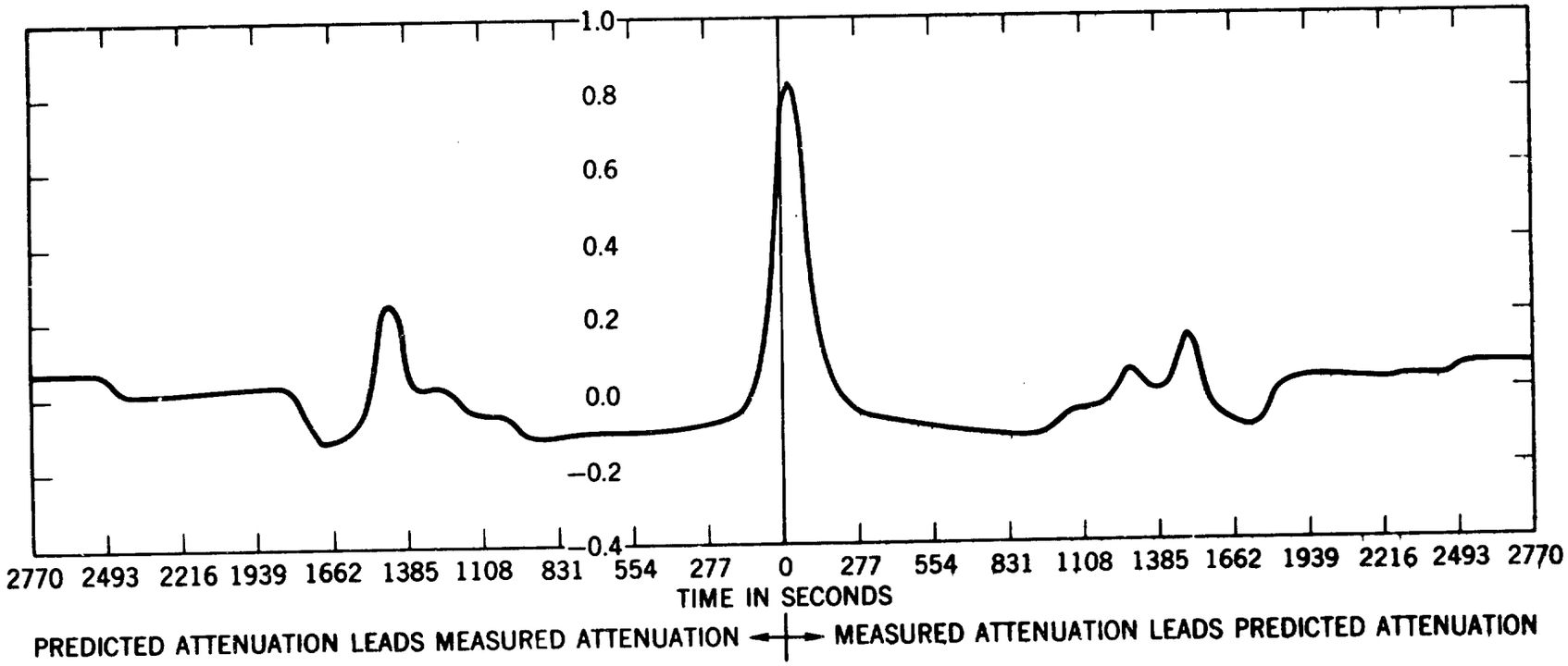

Figure 26. Cross-Covariance Coefficient of Measured 15.3 GHz Attenuation with Attenuation Predicted from 16 GHz Sky Temperature, Day 92, April 2, 1970, 1145-1245 GMT

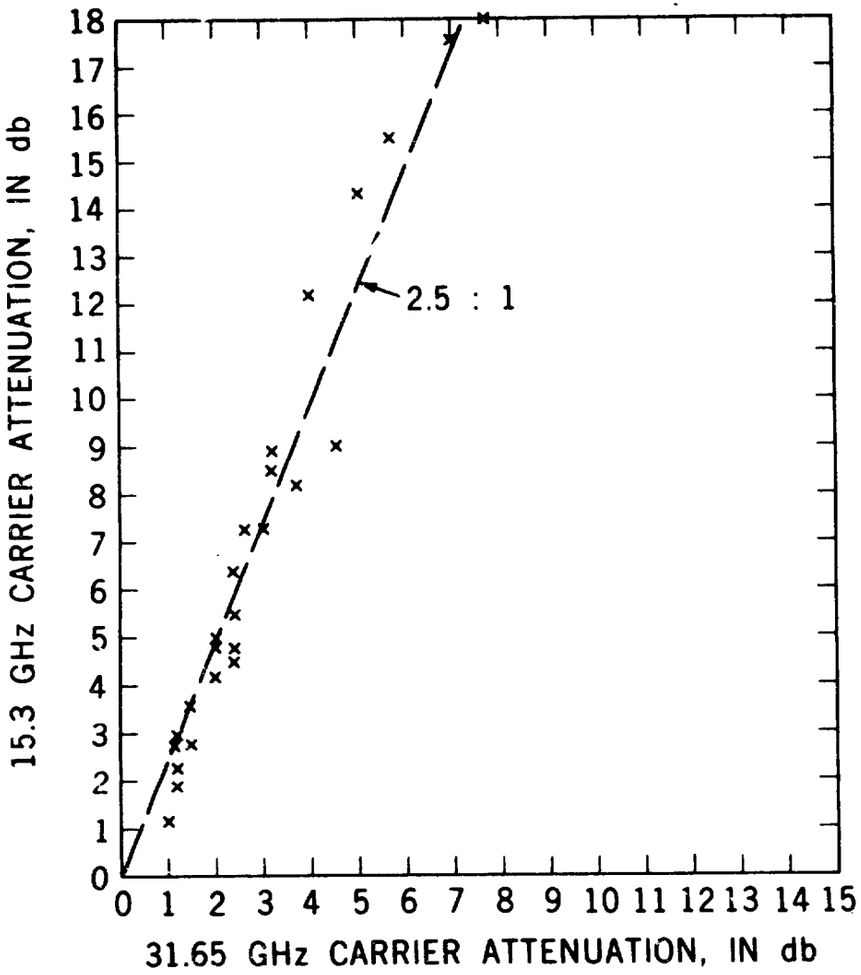

Figure 27. Uplink-Downlink Attenuation Comparison
Day 167, June 16, 1970, 2000 to 2300 GMT WC-7 (Continuous Rain)

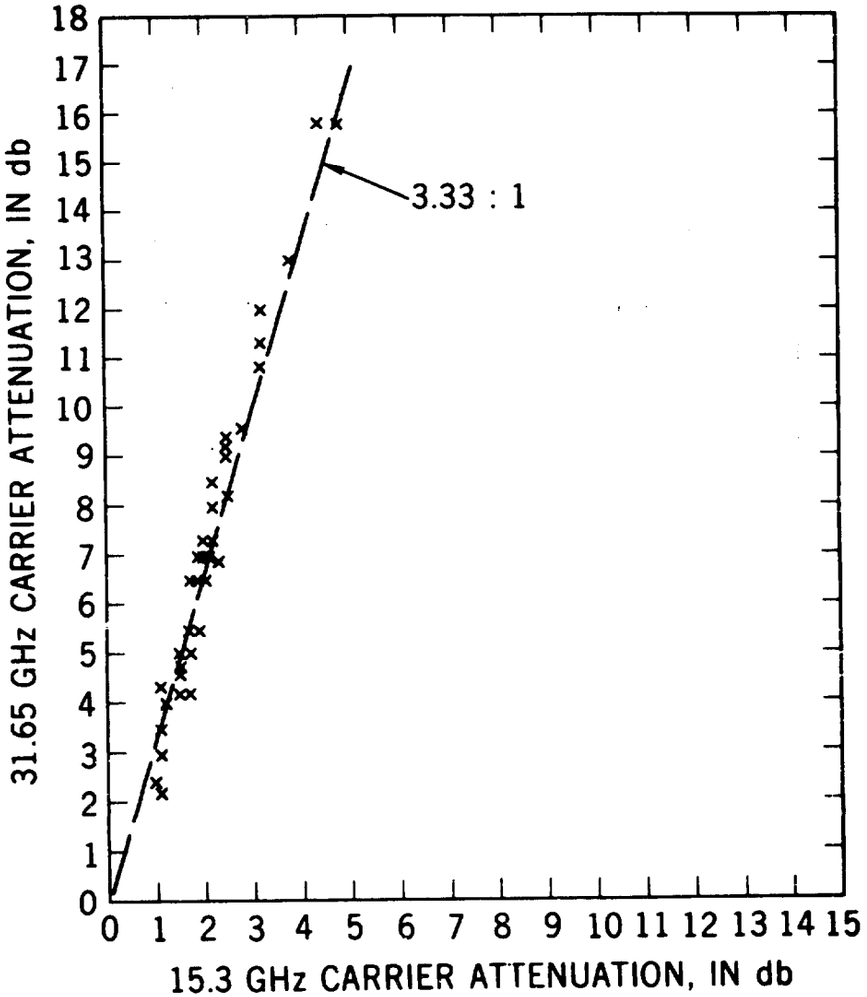

Figure 28. Uplink-Downlink Carrier Attenuations, Day 231
Aug. 19, 1970, 1750-1905 GMT WC-7 (Continuous Rain)

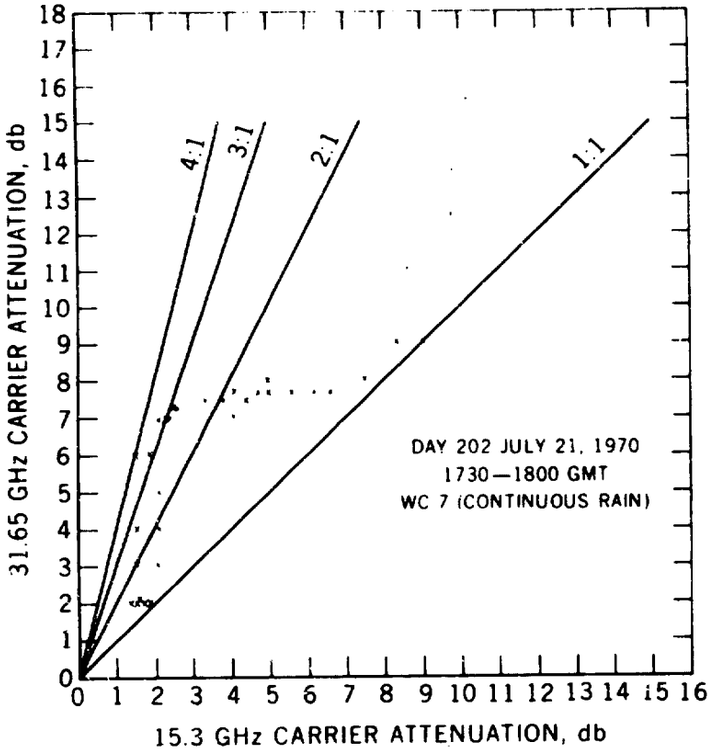

Figure 29. Uplink/Downlink Carrier Attenuations

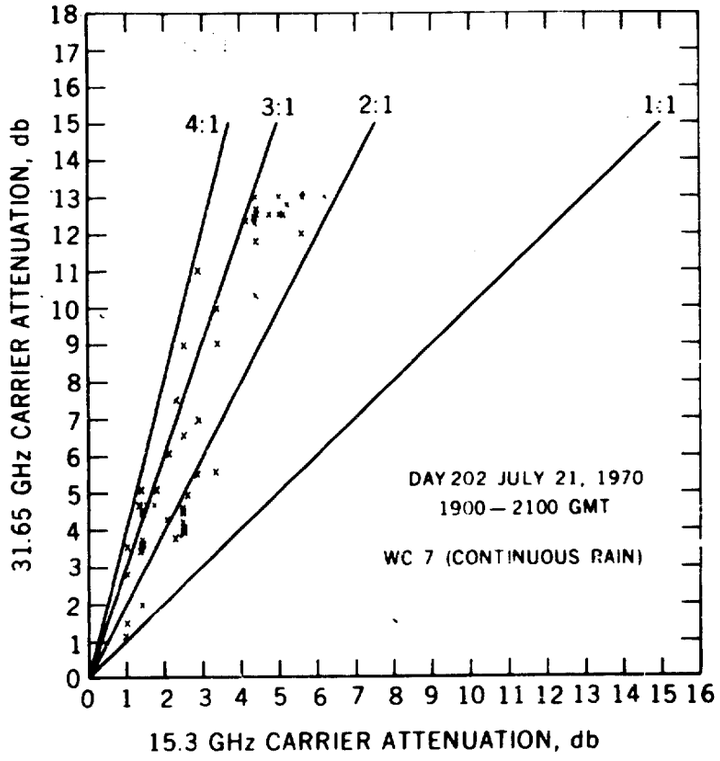

Figure 30. Uplink/Downlink Carrier Attenuations

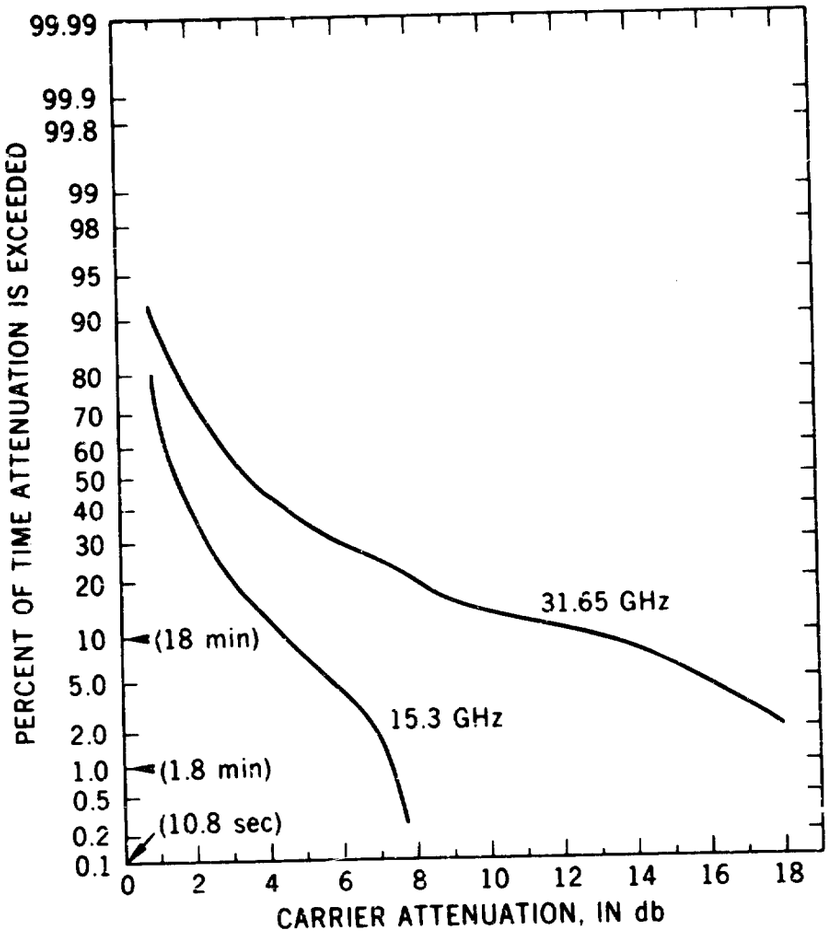

Figure 31. Cumulative Distributions Uplink and Downlink During Rainstorm, Day 167, June 16, 1970, 2000 to 2300 GMT

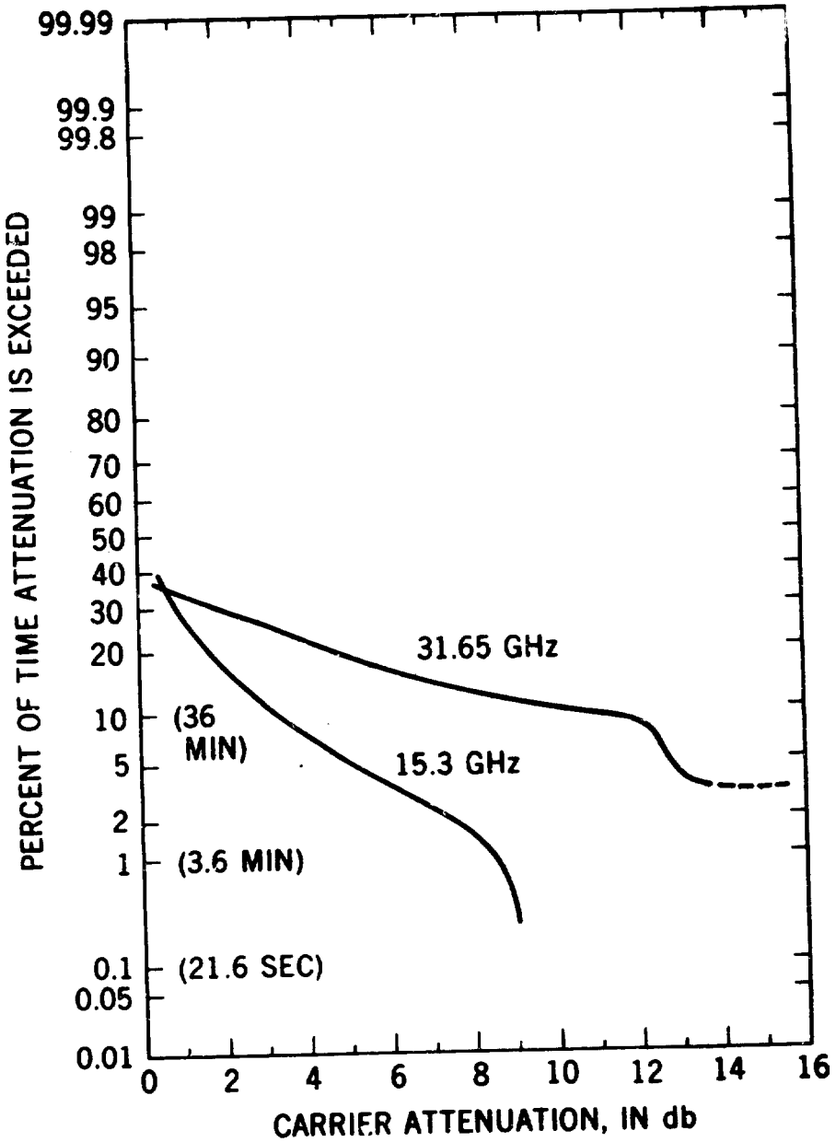

Figure 32. Cumulative Distributions Uplink and Downlink During Rainstorm, Day 202, July 21, 1970, 1730 to 2330 GMT

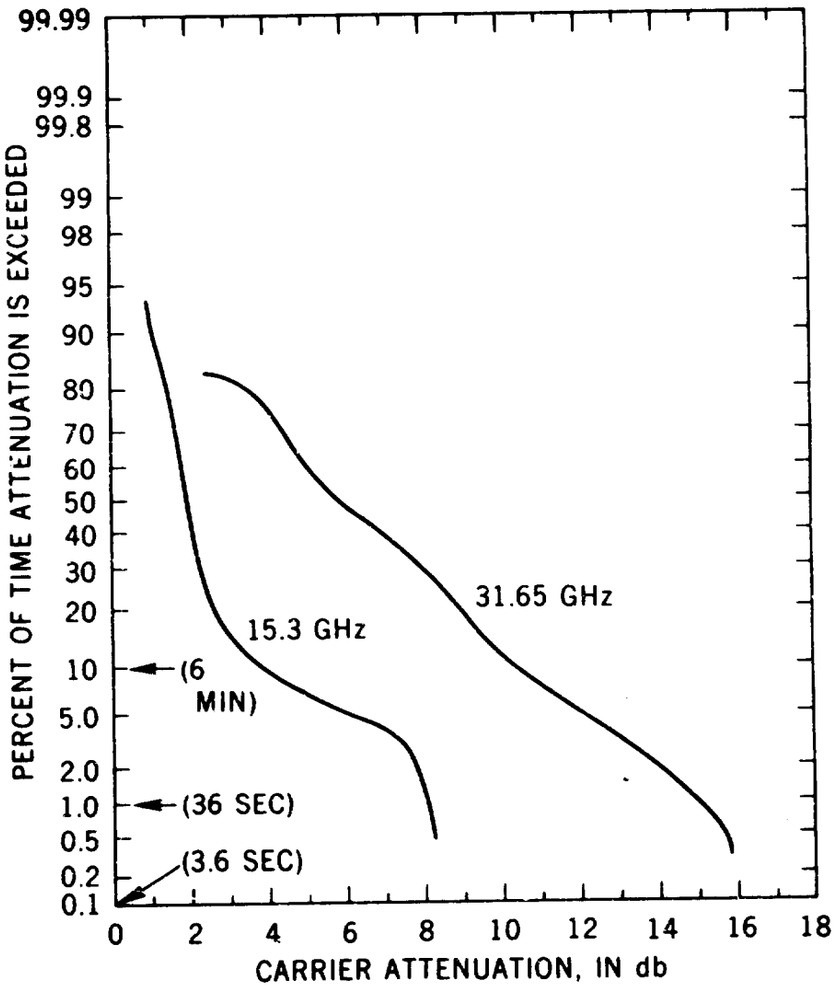

Figure 33. Cumulative Distributions Uplink and Downlink During Rainstorm, Day 231, August 19, 1970, 1750 to 1850 GMT

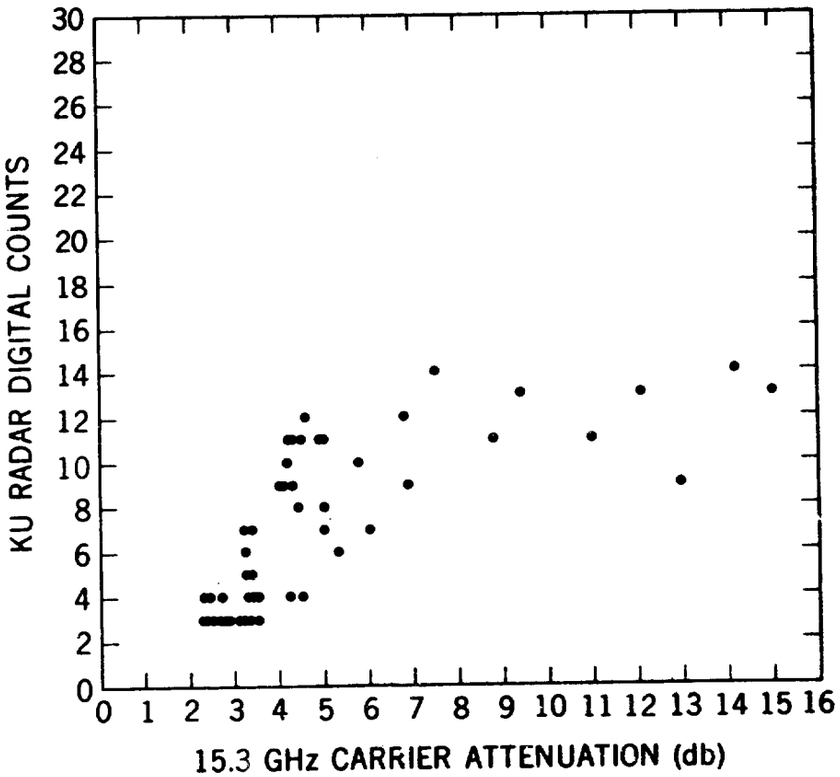

Figure 34. Radar Counts vs. Carrier Attenuation Plot Day 155, June 4, 1350 to 1450 GMT

had similar 15.3 GHz attenuation distributions, exhibited 31.65 GHz distributions which were quite different.

2.4 Other Measurements

Two 15.6 GHz weather radars are in operation at Rosman. One unit is in a vertical scan mode in the azimuth direction of the ATS-V satellite and has been used to locate and measure storm height, cell size, and general weather characteristics. It has two ranges of operation, 8 and [illegible] miles.

The second radar is in an integrated backscatter mode with no scan. The antenna is pointed up the earth-satellite path, and has a beamwidth of 4°. The radar backscatter is displayed in digital counts (0. to 5 volts equals 0 to 63 counts). The returns from 80 radar pulses are combined in each integration period of 100 milliseconds, with a variable range gate adjustable from 1 to 16 kilometers.

Correlation plots of radar backscatter with 15.3 GHz measure attenuation for three storms are shown in Figures 34 through 36. Repeatable trends are not apparent in the results, as further evidenced by the time plots of the storms (Figures 10 through 12). A number of factors will contribute to the lack of point-by-point radars backscatter correlation with signal attenuation. The most significant are: (a) the attenuation experienced at this wavelength limits the penetration capability of the radar signal, (b) the increased beamwidth of the small aperture radar system will enclose a larger storm volume than the satellite antenna beam, and (c) the radar signal is more sensitive to drop size variations, especially at the higher rain intensities.

Radar measurements at longer wavelengths with smaller beamwidths would be expected to exhibit better correlation with attenuation measurements, and this has been demonstrated with ATS-V data at another station location (Reference V-1, Appendix A).

Other measurements made at Rosman include cloud cover photos, weather class designations, wind vector vs. attenuation dispersion, and standard weather parameters (References VII-1, 2, Appendix A).

3.0 SUMMARY

Table 3 presents a summary of data measurements made at the Rosman Station through August 1970.

The [illegible] GHz downlink has been in operation at Rosman since October 1969. A total of 674 hours of propagation data has been recorded with 73 precipitation

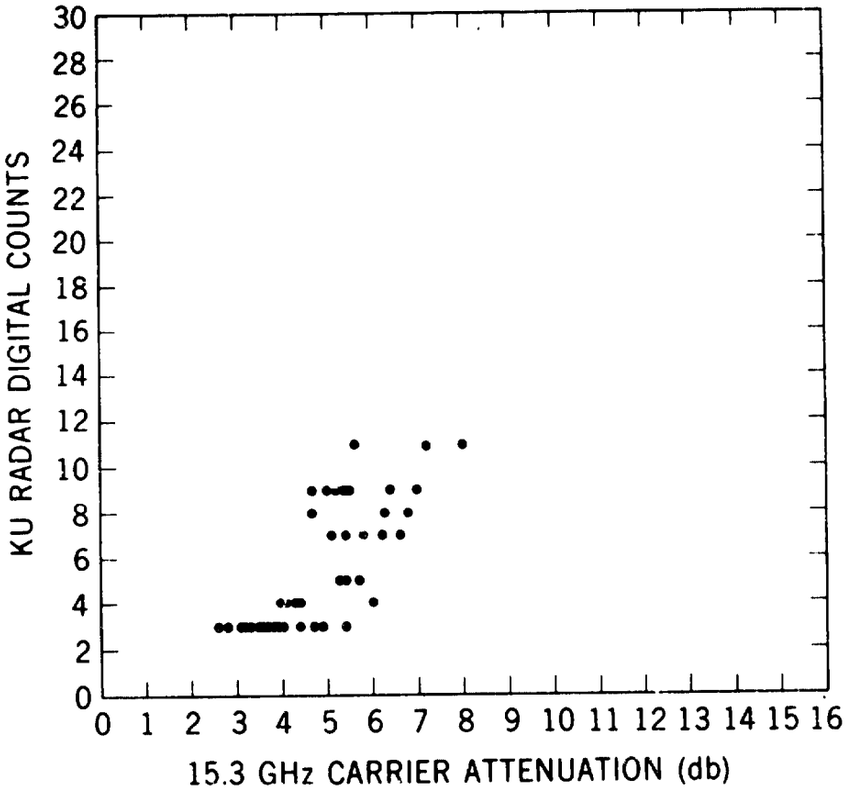

Figure 35. Radar Counts vs. Carrier Attenuation Plot
Day 155, June 4, 1700 to 1730 GMT

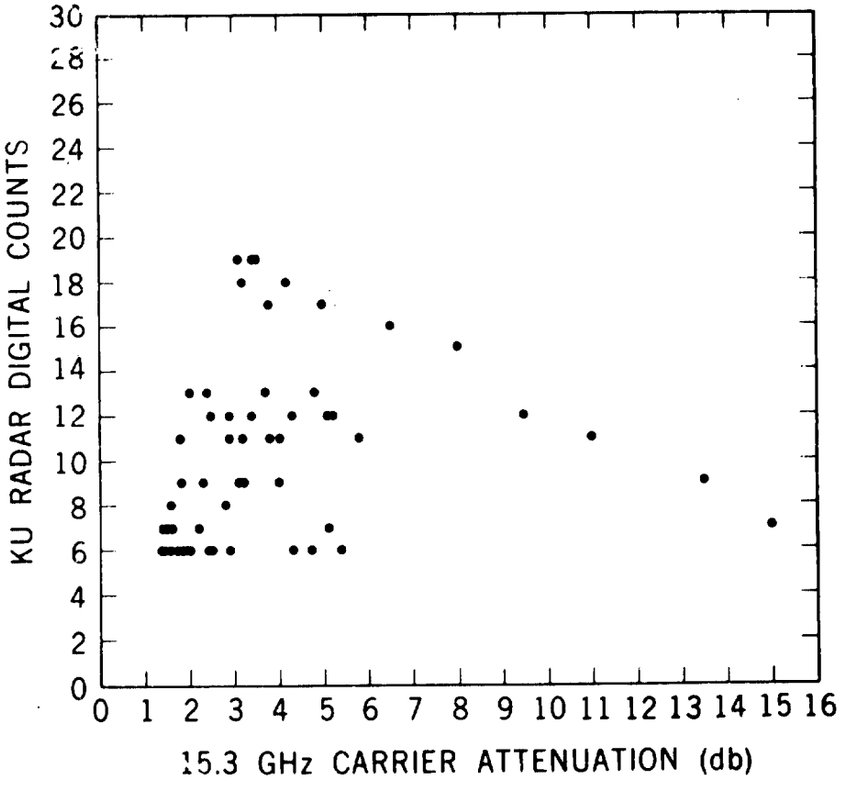

Figure 36. Radar Counts vs. Carrier Attenuation Plot
Day 156, June 5, 1710 to 1810 GMT

Table 3
Measurements Summary ATS-5 Millimeter Wave Experiment
Rosman, N.C. Station, Nov. 1, 1969 to Aug. 31, 1960

15.3 GHz DOWNLINK
- 674 HRS OF OPERATION
- 73 PRECIPITATION OCCURRENCES
- ATTENUATION EXCEEDED 15db FOR 16 MINUTES
- LIMITED SIDEBAND DATA SHOWS NO EFFECTS

31.65 GHz UPLINK
- 127 HRS OF OPERATION
- 24 PRECIPITATION OCCURRENCES
- ATTENUATION EXCEEDED 18db FOR 4 MINUTES
- SIDEBAND AMPLITUDE VARIATIONS WITHIN MEASUREMENT ACCURACY

RAINFALL RATE CORRELATIONS (DOWNLINK)
- LOW FOR SINGLE GAUGE
- SIGNIFICANT IMPROVEMENT WITH HEIGHT AVERAGING
- MEASURED ATTENUATION HIGHER THAN PREDICTED FROM AVERAGED RAINFALL RATES

SMALL APERTURE SKY TEMPERATURE CORRELATIONS (DOWNLINK)
- VERY GOOD FOR MOST STORMS, C_k= 0.6 OR BETTER
- VALID PREDICTIONS TO 15db OF ATTENUATION
- MEASURED ATTENUATION SLIGHTLY LOWER THAN PREDICTED FROM T_s

INTEGRATED K_u BACKSCATTER CORRELATION (DOWNLINK)
- LOW, RESPONSE VARIES WITH EACH STORM

UPLINK – DOWNLINK COMPARISON
- ATTENUATION RATIO STORM & TIME VARIABLE
- 2:1 TO 4:1 RANGE

occurrences. The measurements typically show attenuations of 1 to 3 db in light rains or dense fog; 3 to 7 db in continuous rains (5 to 50 mm/hr), and a number of fades exceeding 12 db in heavy thunderstorms.

The maximum attenuation of 15 db was exceeded on four separate occasions for a total time of 16 minutes. Single rain gauge readings up to 76.2 mm/hr were recorded, with ground average rates in excess of 70 mm/hr and height averaged rates near 50 mm/hr. during these periods.

Limited sideband data obtained before transmitter power degradations showed no decorrelation effects in amplitude or relative sideband phase.

The 31.65 GHz uplink has been in operation for 127 hours since December 1969 with 24 precipitation occurrences.

Attenuation exceeded 18 db for a total of 4 minutes. Sideband measurements at ±50, ±10, and ±1 MHz have shown relative amplitude variations within ±2 db over most periods but with no increase during precipitation events.

Correlation of measured attenuation with ground measured rainfall rate was low for a single gauge but improved significantly with height averaging of ten rain gauges with both uplink and downlink data.

In most instances the measured attenuation was slightly higher than that predicted from the averaged rainfall rates.

If these trends continue with future data, it appears that the utilization of ground measured rainfall rate data may be of some use in predicting earth-satellite path propagation when only long-term or gross effects are desired, such as in outage time predictions for a specific location.

The utilization of rainfall data to evaluate short term attenuation statistics, such as is required for diversity studies, appears quite limited.

It is apparent that more than one gauge is required, however, and that height averaging techniques must be employed to reduce the errors introduced by the increasing distance between the earth-satellite path and the measuring device on the ground.

Correlations of measured attenuation with sky temperature recorded with a small aperture radiometer were very good for the great majority of storms. (There were a small number of uncorrelated periods observed, however.)

Valid predictions of attenuation from 16 GHz sky temperature measurements were observed for up to 15 db of measured downlink attenuation. In most instances the measured attenuation was slightly lower than that predicted from the sky temperature.

Correlation of measured attenuation with 15.6 GHz backscatter from a small aperture weather radar has been low, with the response varying with each storm. No repeatable trends have been observed.

The uplink to downlink attenuation ratio varied with each precipitation event and often varied during a single storm period. The ratio has ranged from 2:1 to 4:1 during heavy precipitation periods.

Present plans call for ATS-V operations through June of 1971. A complete evaluation of the propagation statistics in the two frequency bands under investigation must await the reduction and analysis of the complete weather

profile data at the Rosman station. From the data reduced to date, however, it appears that both frequency bands exhibit an excellent potential for eventual utilization in reliable high data rate earth-space communications systems.

REFERENCES

1. Binkley, Ippolito, King, and Ratliff, The ATS-E Millimeter Wave Propagation Experiment, April 1968, NASA/GSFC Report X733-68-196.

2. Ippolito, Louis J., ATS-V Millimeter Wave Experiment Data Report, October-December 1969, March 20, 1970, NASA/GSFC Report X-733-70-123.

3. Ippolito, Louis J., Millimeter Wave Propagation Measurements from the Applications Technology Satellite (ATS-V), IEEE Trans. on Antennas and Propagation, July 1970, pg. 525-552.

4. Straiton, A. W., Bailey, C. R., and Vogel, W., Amplitude Variations of 15 GHz Radio Waves Transmitted Through Clear Air and Through Rain, Radio Science, Vol. 5, No. 3, pg. 551-557, March 1970.

5. Straiton, A. W., and Fannin, B. M., Comparison of 15 GHz Propagation Data from the ATS-V Satellite with Ground Based Radio and Meteorological Data, for presentation to the NATO-AGARD Electromagnetic Wave Propagation Panel, September 1970, Dusseldorf, Federal Republic of Germany.

6. Penzias, A. A., First Result from 15.3 GHz Earth-Space Propagation Study The Bell System Technical Journal, July-August 1970, pg. 1242-1245.

7. Biuge, A., Levatich, J., and Robertson, E., COMSAT Laboratories, Clarksburg, Maryland, Propagation Experiment above 10 GHz for Application to Communications Satellite System, presented at the AIAA 3rd Communications Satellite Conference, April 8, 1970, Los Angeles, Calif.

8. B. C. Blevis, R. M. Dohoo, and K. C. McCormick, "Measurements of Rainfall Attenuation at 8 and 15 GHz," IEEE Trans. Antennas Propagation Vol. AP-15, pp. 394-403, May 1967.

9. R. G. Medhurst, "Rainfall Attenuation of Centimeter Waves: Comparison of Theory and Measurement," IEEE Trans. Antennas Propagation, Vol. AP-13, pp. 550-564, July 1965.

10. C. W. Tolbert, A. W. Straiton, and C. O. Britt, "Propagation Studies Between 18.0 and 25.5 kmcs," Elec. Engrg. Res. Lab., University of Texas, Austin, Rept. 110, July 1959.

11. K. Funakawa, T. Kido, K. Kitamura, Y. Otsu, T. Katto, and M. Uratsuka, "Propagational Experiments of 13 GHz and 35 GHz over the 80 kM Path," J. Radio Res. Lab. Jap., Vol. 14, pp. 249-265, November 1967.

12. K. L. S. Gunn and T. W. R. East, "The Microwave Properties of Precipitation Particles," J. Royal Meteorol. Sec., Vol. 80, pp. 522-555, 1954.

13. K. N. Wulfsberg, "Apparent Sky Temperatures at Millimeter Wave Frequencies," Phys. Sci. Res. Papers, AFCRL, July 1964.

APPENDIX A

DATA REPORTS ON THE ATS-V MILLIMETER WAVE EXPERIMENT

Listed below are reports and presentations on the data results of the ATS-V Millimeter Wave Experiment from the participating stations available through September, 1970.

I. NASA-ROSMAN, North Carolina

I-1. Ippolito, Louis J., ATS-V Millimeter Wave Experiment Data Report, October-December 1969, March 20, 1970, NASA/GSFC Report X-733-70-123.

I-2. Ippolito, Louis J., Millimeter Waves for Domestic Satellite Systems, presented at AIAA 3rd Communications Satellite Systems Conference, Los Angeles, Cal., April 7, 1970.

I-3. Ippolito, Louis J., Millimeter Waves for Space Communications, presented at the IEEE 1970 International Conference on Communications, San Francisco, Cal., June 9, 1970.

I-4. Ippolito, Louis J., Millimeter Wave Propagation Measurements from the Applications Technology Satellite (ATS-V), IEEE Trans. on Antennas and Propagation, July 1970, pg. 525-552.

I-5. Ippolito, L. J., Propagation Statistics for 15 and 32 GHz Earth-Space Transmissions from the Applications Technology Satellite (ATS-V), presented at the Fall 1970 USNC/URSI Meeting, Columbus Ohio, Sept. 15, 1970.

II. University of Texas, Austin, Texas

II-1. Straiton, A. W., and Fannin, B. M., Comparison of 15 GHz Propagation Data from the ATS-V Satellite with Ground Based Radio and Meteorological Data, for presentation to the NATO-AGARD Electromagnetic Wave Propagation Panel, September 1970, Dusseldorf, Federal Republic of Germany.

II-2. Fannin, B. M., Straiton, A. W., Pate, D. N., Effects of Rain on Earth-Satellite Path at 15 GHz, presented at the Fall 1970 USNC/URSI Meeting, Columbus, Ohio, September 15, 1970.

III. Ohio State University, Columbus, Ohio

III-1. Bohley, P., Hodge, D. B., A Millimeter Wave Diversity Propagation Experiment, presented at the Fall 1970 USNC/URSI Meeting, Columbus, Ohio, September 15, 1970.

IV. COMSAT/INTELSAT, Clarksburg, Maryland

IV-1. Biuge, A., Levatich, J., and Robertson, E., COMSAT Laboratories, Clarksburg, Maryland, Propagation Experiment above 10 GHz for Application to Communications Satellite System, presented at the AIAA 3rd Communications Satellite Conference, April 8, 1970, Los Angeles, Calif.

IV-2. Buige, A., Craft, H. Jr., Levatich, J., Robertson, E., Millimeter Wave Propagation Measurements with ATS-5 at COMSAT Labs., presented at the Fall 1970 USNC/URSI Meeting, Columbus, Ohio, September 15, 1970.

V. Communications Research Centre, Ottawa, Canada

V-1. Strickland, J. I., Attenuation, Emission and Backscatter by Precipitation, presented at the Fall 1970 USNC/URSI Meeting, Columbus, Ohio, Sept. 15, 1970.

VI. Bell Telephone Labs, Holmdel, New Jersey

VI-1. Penzias, A. A., First Result from 15.3 GHz Earth-Space Propagation Study, The Bell System Technical Journal, July-August 1970, pg. 1242-1245.

VI-2. Penzias, A. A., Propagation Data from Crowford Hill, presented at the Fall 1970 USNC/URSI Meeting, Columbus, Ohio, September 15, 1970.

VII. NASA Participating Stations (Rosman, O.S.U., U. of T. and NELC)

VII-1. ATS Technical Data Report, Quarterly Input, July 6, 1970, prepared for NASA/GSFC by Westinghouse Electric Corp., Contract NAS 5-21129, Section 7.3.

VII-2. ATS Technical Data Report, Quarterly Input September 21, 1970, prepared for NASA/GSFC by Westinghouse Electric Corp., Contract NAS 5-21129, Section 7.3.